Localized electron states on the liquid helium surface as qubits

P. D. Grigoriev

Landau Institute for Theoretical Physics, Chernogolovka, Russia

The National University of Science and Technology MISiS, Moscow

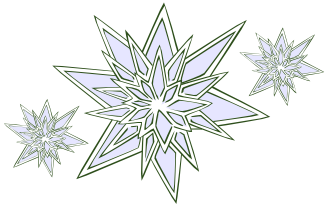

Outline of the talk

1. Introduction on qubits and quantum computing
2. Introduction on surface electrons above liquid He
3. Qubits based on electrons on liquid He surface (theory):

   (a) vertical and horizontal level quantization for localized electron states on the liquid helium surface; their transition line broadening and decoherence; possible read-out configurations.

   (b) spin of electrons above He surface as qubit;

   (c) Negative ions on the helium surface as qubits.
3. Experimental achievements with electrons above liquid He.

Burevestnik, September, 2016

Quantum bit

The simplest qubit - a single quantum particle with spin ½

Classical bit

0 1

n classical bits contain information of one integer number with value ~2^n.

Quantum bit (qubit)

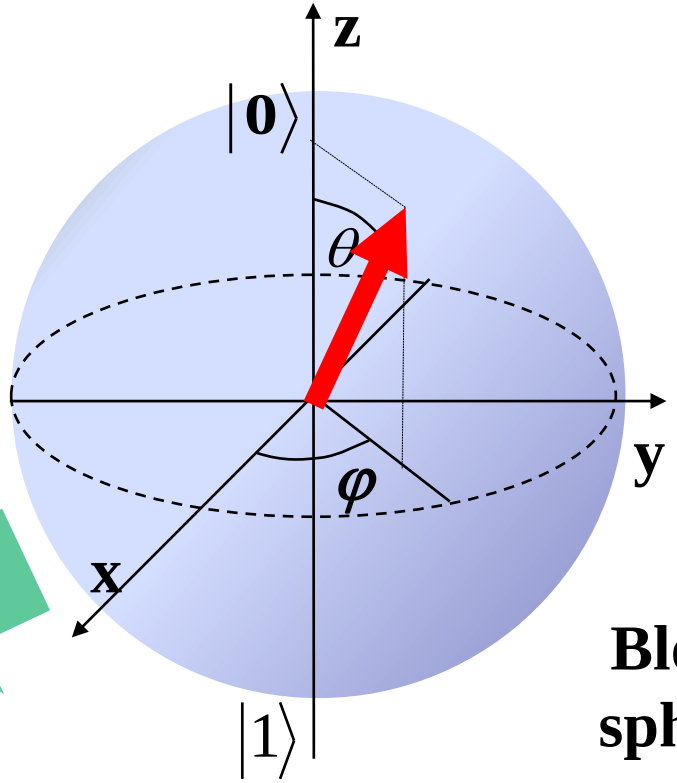

Wave function

$$|\Psi\rangle = \alpha|0\rangle + \beta|1\rangle$$

Bloch sphere

System of n qubits is described by the vector

$$|\psi\rangle = \sum_{x=0}^{2^n-1} a_x |x\rangle$$

and contains information of 2^n complex numbers !

Quantum computer ≠ analogue computer

В ходе квантовых вычислений интерференция амплитуд происходит повсеместно и автоматически. Поэтому некоторые авторы представляют себе квантовый компьютер как сложный интерферометр для амплитуд вектора состояния квантового компьютера.

Это не верно!

в КК 2^n интерференций!

В оптическом компьютере происходит однократная интерференция оптических мод E_j; в квантовом компьютере происходит 2^n-кратная интерференция амплитуд для каждого вектора $|x\rangle$, $0 \leqslant x \leqslant 2^n - 1$. Вектор состояния квантового компьютера содержит как цифровую ($|x\rangle$), так и аналоговую (a_x) информацию; оптический компьютер содержит только аналоговую (E_j) информацию. Оптический компьютер не способен моделировать квантовые вычисления, он должен быть отнесен к классу классических аналоговых компьютеров.

$$\sum_{j=1}^{l} E_j = \sum_{j=1}^{l} a_j \sin(\omega t + \varphi_j), \qquad \sum_{j=1}^{l} |\psi_j\rangle = \sum_{j=1}^{l} \sum_{x=0}^{2^n-1} a_x^{(j)} |x\rangle = \sum_{x=0}^{2^n-1} \left(\sum_{j=1}^{l} a_x^{(j)} \right) |x\rangle$$

System of n qubits

is described by the vector $|\psi\rangle = \sum_{x=0}^{2^n-1} a_x |x\rangle$

States superposition-> parallelism: change of one qubit changes the superposition of all 2^n states

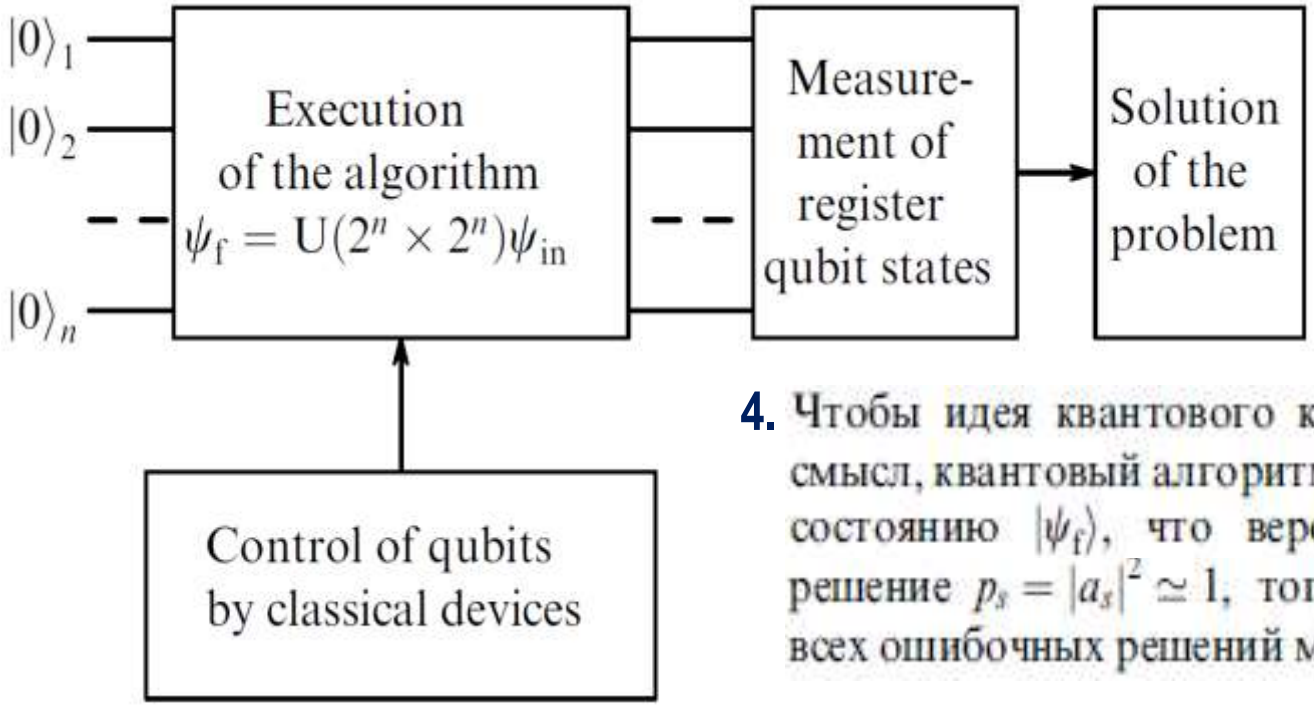

Схема квантового компьютера

Quantum computer needs:

1. Long time of quantum coherence (no errors).
2. Controllable interaction between qubits.
3. Read-out of final state.

4. Чтобы идея квантового компьютера имела реальный смысл, квантовый алгоритм должен приводить к такому состоянию $|\psi_f\rangle$, что вероятность найти правильное решение $p_s = |a_s|^2 \simeq 1$, тогда как сумма вероятностей всех ошибочных решений мала: $\sum_{x \neq s} |a_x|^2 \ll 1$

Все придуманные к настоящему времени квантовые алгоритмы обладают описанным свойством. Итак, квантовый компьютер дает цифровое решение задачи s с определенной вероятностью, т.е. является цифровым вероятностным компьютером.

Method of realization of quantum algorithm

Управление работой квантового компьютера с n кубитами описывает преобразование $|\psi_f\rangle = U(2^n \times 2^n)|\psi_{in}\rangle$, где $|\psi_{in}\rangle$ и $|\psi_f\rangle$ — векторы с 2^n компонентами. При значениях $n = 10^3$ умножение $U|\psi_{in}\rangle$ становится недоступным для самых быстрых (порядка 10^{12} операций в секунду) компьютеров. Еще более трудной представляется физическая реализация преобразования U

Путь к реализации квантовых алгоритмов обнаруживается, если рассмотреть возможность разложения матрицы $U(2^n \times 2^n)$ в упорядоченное произведение матриц второго и четвертого порядков: $U(2^n \times 2^n) = \prod_{i,j} U_i(2 \times 2) \otimes U_j(2^2 \times 2^2)$

Однокубитовые операции описывают вращение отдельного кубита: $\alpha|0\rangle + \beta|1\rangle \rightarrow \alpha'|0\rangle + \beta'|1\rangle$

Из 2-кубитовых операций достаточно одной CNOT:

Input state	$\|00\rangle$	$\|01\rangle$	$\|10\rangle$	$\|11\rangle$
Output state	$\|00\rangle$	$\|01\rangle$	$\|11\rangle$	$\|10\rangle$

$|\psi_1\rangle = \alpha_1|0\rangle + \beta_1|1\rangle$, $|\psi_2\rangle = \alpha_2|0\rangle + \beta_2|1\rangle$, $\Rightarrow$ $|\psi_{12}\rangle = \alpha_1\alpha_2|00\rangle + \alpha_1\beta_2|01\rangle + \beta_1\alpha_2|11\rangle + \beta_1\beta_2|10\rangle$

Quantum algorithms, faster than classical

Three classes of quantum algorithms have been discovered and comprehensively investigated: (1) algorithms with quantum hidden subgroups of the Abelian transformation group (among them is Shor's number factorization algorithm [1994]); (2) algorithms with amplitude amplification (represented by Grover's algorithm for object search in an unstructured database [1996]); (3) algorithms for modeling quantum systems with a quantum computer.

Class-(1) and (3) algorithms apply a discrete Fourier transformation. Performing the Fourier transformation with a classical computer requires an exponentially large number of operations. With a quantum computer, the Fourier transformation is performed in a polynomial number ~n^2 of operations. That is why class-(1) and (3) algorithms demonstrate an exponential acceleration in comparison with the algorithms executed with classical computers.

The principle of Grover's algorithm is the amplitude amplification of the state corresponding to the desired object. It gives only $n^{1/2}$ acceleration.

Безопасность передачи данных

Безопасность передачи данных основана на протоколе RSA (электронные платежи, PIN-коды, шифрование e-мэйл, и т.п.)

R. Rivest, A. Shamir, and L. Adleman, "*A method for Obtaining Digital Signatures and Public-Key cryptosystems*" (1977)

Протокол RSA использует асимметрию двух задач:

легкая задача: умножение 77236 x 42231 = 3261753516

трудная задача: разложение 48151623427 = ? x ?

пример (упрощенно):

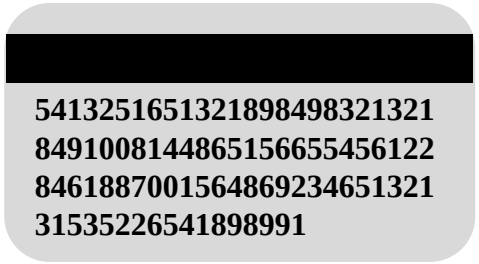

кредитная карта содержит длинное число Z - "Public Key"

+

Вы вводите PIN-код - "Private Key"

Банкомат проверяет, делится ли число Z на PIN-код

Если делится – ОК !

Quantum teleportation algorithms

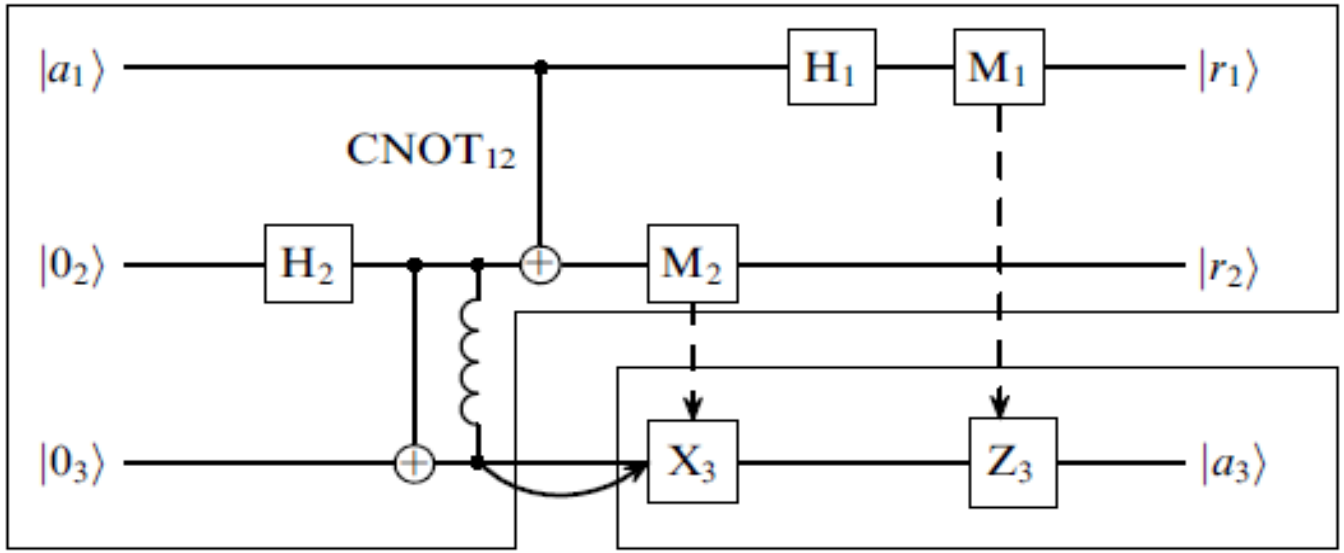

Schematic protocol of teleportation of an unknown state from point A to point B. Entanglement is produced in the course of teleportation and is later destroyed during qubit state measurements. In addition, one of the qubits of the entangled pair is transported from point A to point B.

One-qubit operations:

1. Hadamard operation

$$\mathrm{H} = \frac{1}{\sqrt{2}}\begin{pmatrix} 1 & 1 \\ 1 & -1 \end{pmatrix} = \frac{1}{\sqrt{2}}(\mathrm{X} + \mathrm{Z})$$

$$\mathrm{H}\begin{vmatrix} 1 \\ 0 \end{vmatrix} = \frac{1}{\sqrt{2}}(|0\rangle + |1\rangle)$$

2.

$$\mathrm{X}\begin{vmatrix} a \\ b \end{vmatrix} = \begin{vmatrix} b \\ a \end{vmatrix} = \mathrm{NOT}\begin{vmatrix} a \\ b \end{vmatrix}$$

$$\mathrm{X} = \mathrm{NOT} = \mathrm{R}_x(\pi)$$

3.

$$\mathrm{Z}\begin{vmatrix} a \\ b \end{vmatrix} = \begin{vmatrix} a \\ -b \end{vmatrix}$$

4. M - measurement

Algorithm of quantum teleportation of unknown quantum state

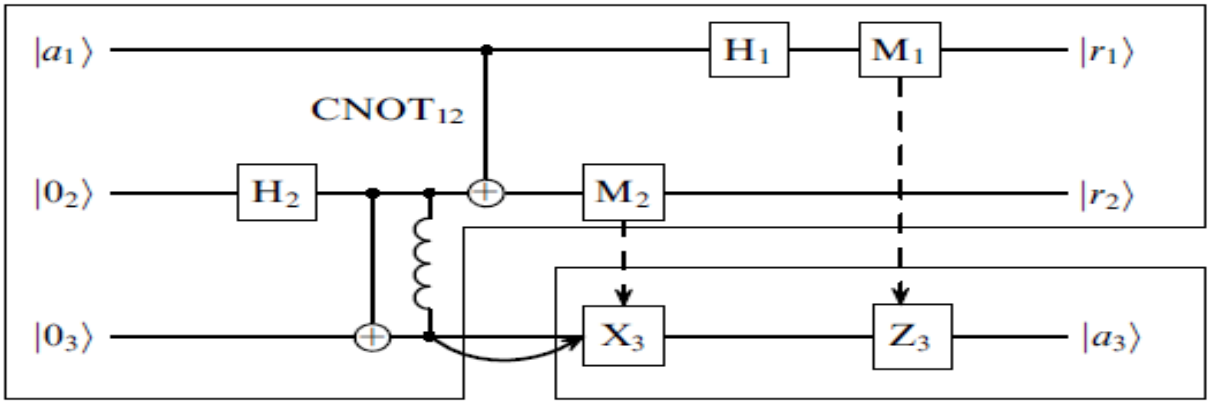

1. В первой операции создается запутанность кубитов 2 и 3

$$|0_2\rangle|0_3\rangle \xrightarrow{H_2} \frac{1}{\sqrt{2}}\left(|0_2\rangle + |1_2\rangle\right)|0_3\rangle \xrightarrow{CNOT_{23}} \frac{1}{\sqrt{2}}\left(|0_2 0_3\rangle + |1_2 1_3\rangle\right)$$

Затем кубит 3 переносится на большое расстояние и больше не участвует в локальных операциях с кубитами 1,2 (заранее заготовленные запутанные кубиты 2,3).

Во 2-й операции запутанность кубитов 2 и 3 преобразуется в запутанность кубитов 1 и 3 с участием всех трех кубитов, измерения кубита 2 и передачи результата по классическому каналу.

$$\frac{1}{\sqrt{2}}\left(\alpha|0_1\rangle + \beta|1_1\rangle\right)\left(|0_2 0_3\rangle + |1_2 1_3\rangle\right) \xrightarrow{CNOT_{12}}$$

$$\xrightarrow{CNOT_{12}} \left(\alpha|0_1 0_2 0_3\rangle + \alpha|0_1 1_2 1_3\rangle + \beta|1_1 1_2 0_3\rangle + \beta|1_1 0_2 1_3\rangle\right)$$

$$\xrightarrow{M_2(|0_2\rangle)} \left(\alpha|0_1 0_3\rangle + \beta|1_1 1_3\rangle\right)|0_2\rangle .$$

Если результат измерения M_2 будет $|1_2\rangle$, то над кубитом 3 выполняется операция X = NOT.

3. Измерение M_2, произведенное над кубитом 2, освободило его от запутанности. Используем еще раз это свойство измерения, чтобы освободить от запутанности кубит 1

$$\left(\alpha|0_1 0_3\rangle + \beta|1_1 1_3\rangle\right)|r_2\rangle \xrightarrow{H_1}$$

$$\xrightarrow{H_1} \left(\alpha|(+)_1 0_3\rangle + \beta|(-)_1 1_3\rangle\right)|r_2\rangle$$

$$\xrightarrow{M_1(|0_1\rangle)} \left(\alpha|0_3\rangle + \beta|1_3\rangle\right)|0_1\rangle|r_2\rangle ,$$

If M1 gives |1>, operation Z is performed on qubit 3

где $(\pm) = |0\rangle \pm |1\rangle$

Decoherence and quantum errors

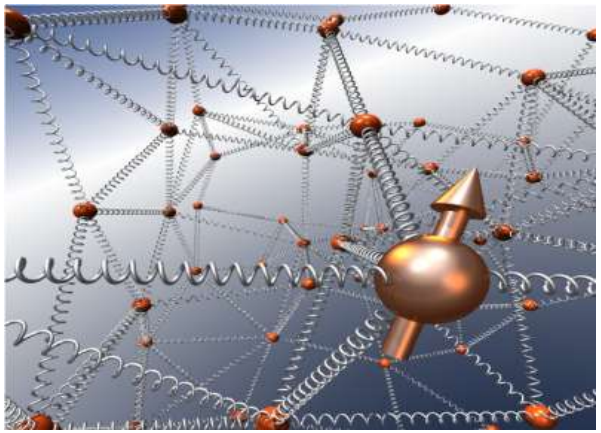

An important parameter of a qubit is the time of decohering τ_{dc} of its states.

The register of L qubits loses its coherence in a shorter time:

$$\tau_{dc}^{L} = \frac{\tau_{dc}}{L^{\alpha}}, \qquad \alpha = 1, 2.$$

The decoherence time τ^{L}_{dc} should be compared with the mean operation time τ_{op}, which is about the period of Rabi oscillations.

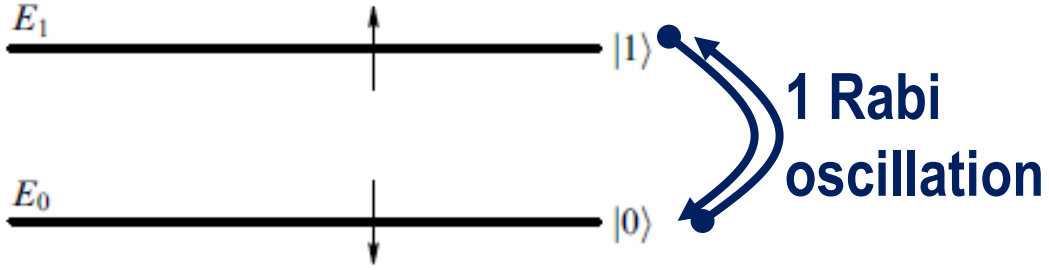

The ratio $\tau_{op} / \tau^{L}_{dc}$ shows how many computational operations can be performed while the quantum computer retains its state coherence.

For instance, Shor's algorithm for L-digit number factorization requires L^3 operations:

$$\frac{\tau_{Shor}}{\tau_{dc}^{L}} = \frac{\tau_{op} L^3}{\tau_{dc} / L^{\alpha}} = \frac{\tau_{op}}{\tau_{dc}} L^{(3+\alpha)}$$

How is it possible to make a useful QC?

Other difficulties: read-off and controllable interaction between qubits.

Quantum error correction

The only invented solution of decoherence problem is the quantum error correction

ln quantum correction protocols the requisite number of qubits and operations is ~10^t, where t is the number of encoding cascades. For single error correction one needs ~10 qubits and operations (while 3 bits are sufficient in classical computer). However, if double errors are possible, one needs ~100 qubits and operations . Error-correction operations themselves introduce additional errors.

The computations are fault-tolerant if the error correction procedures remove more errors from the computer than they introduce.

The quantum computer can operate for an arbitrarily long time if the error probability in one elementary quantum operation is below the threshold value $\varepsilon_{\text{th}} \leqslant 10^{-5} - 10^{-4}$

Types of qubits

photons

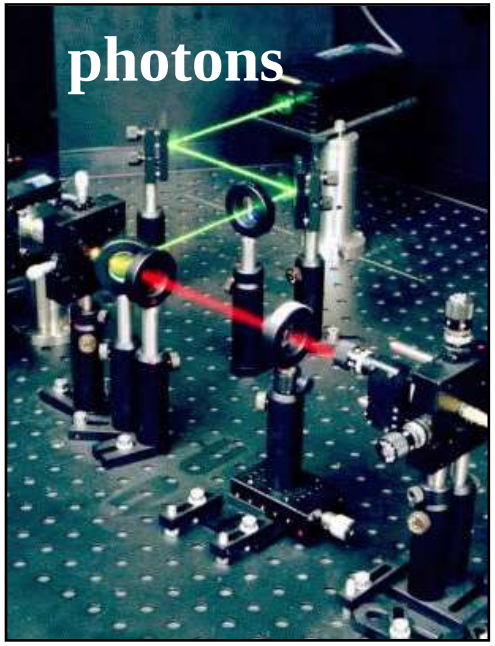

Quantum dots

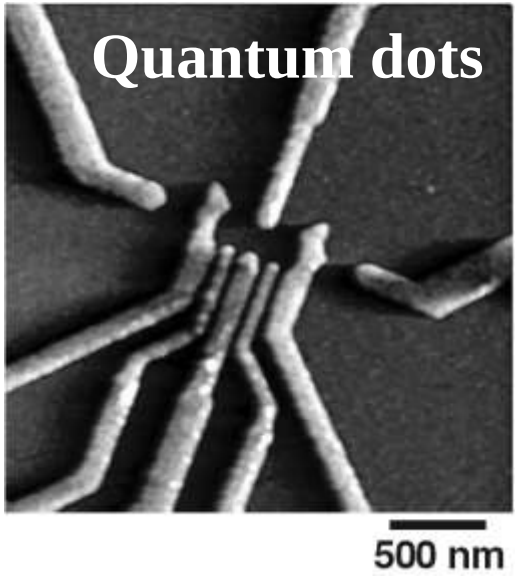

Ions and atoms in trap

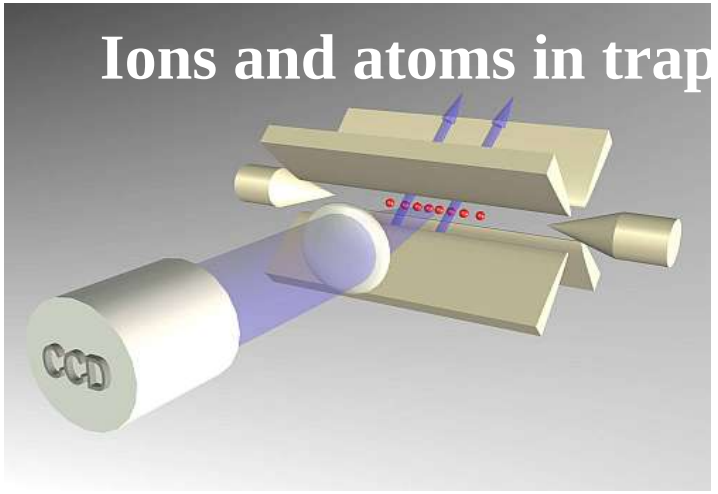

Spins in molecules

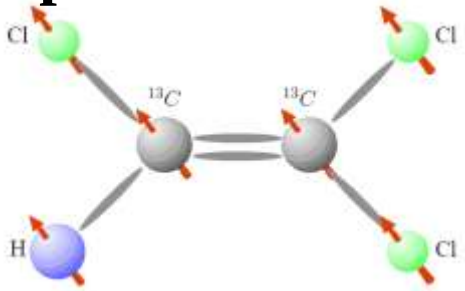

Defects in crystals

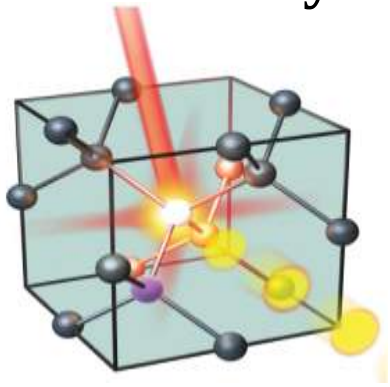

Spins in silicon

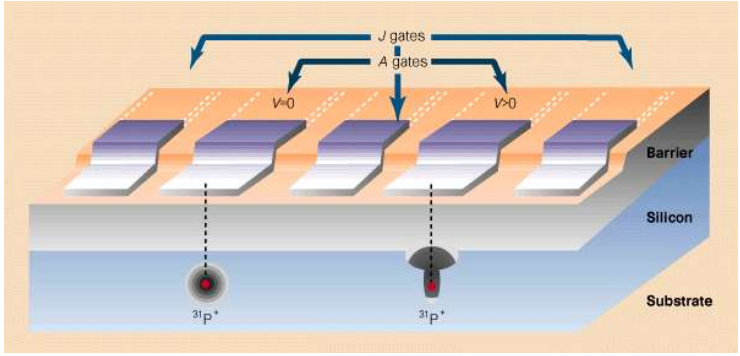

Superconducting qubit

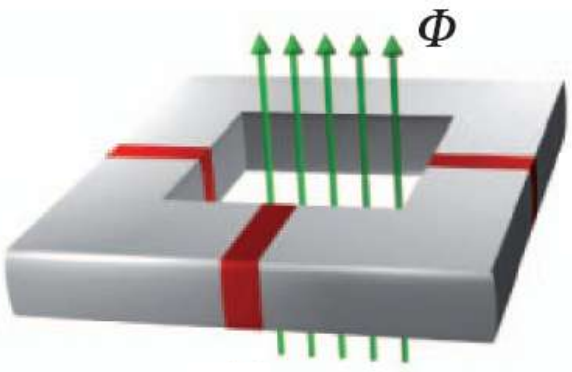

Qubit is a superconducting ring with one or more Josephson junctions

from the point of view of quantum mechanics, the qubit is an artificial system with quantum states $|0\rangle$ and $|1\rangle$

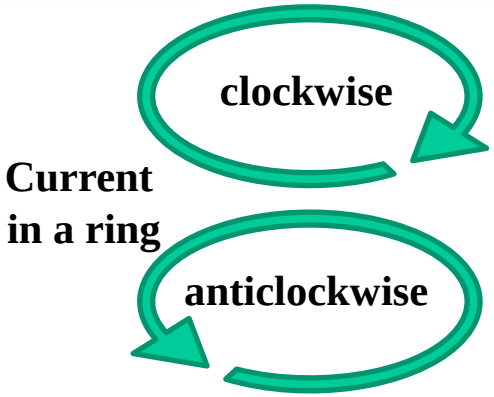

Qubit spectrum

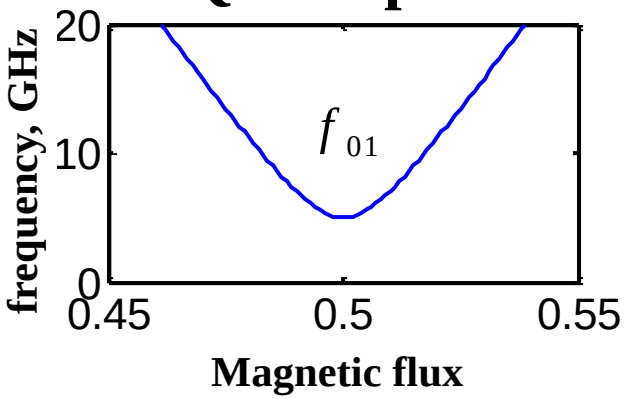

Two-level system

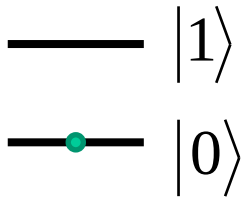

Josephson equation

$$I_S = I_C \sin\varphi$$

$$V = \frac{\Phi_0}{2\pi}\frac{d\varphi}{dt}$$

superconductor
Tunnel barrier
superconductor

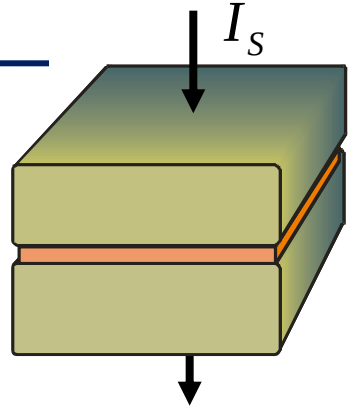

SC qubits lifetime (coherence) : «Moore's law» for superconductors

Qubits lifetime (Nanoseconds)

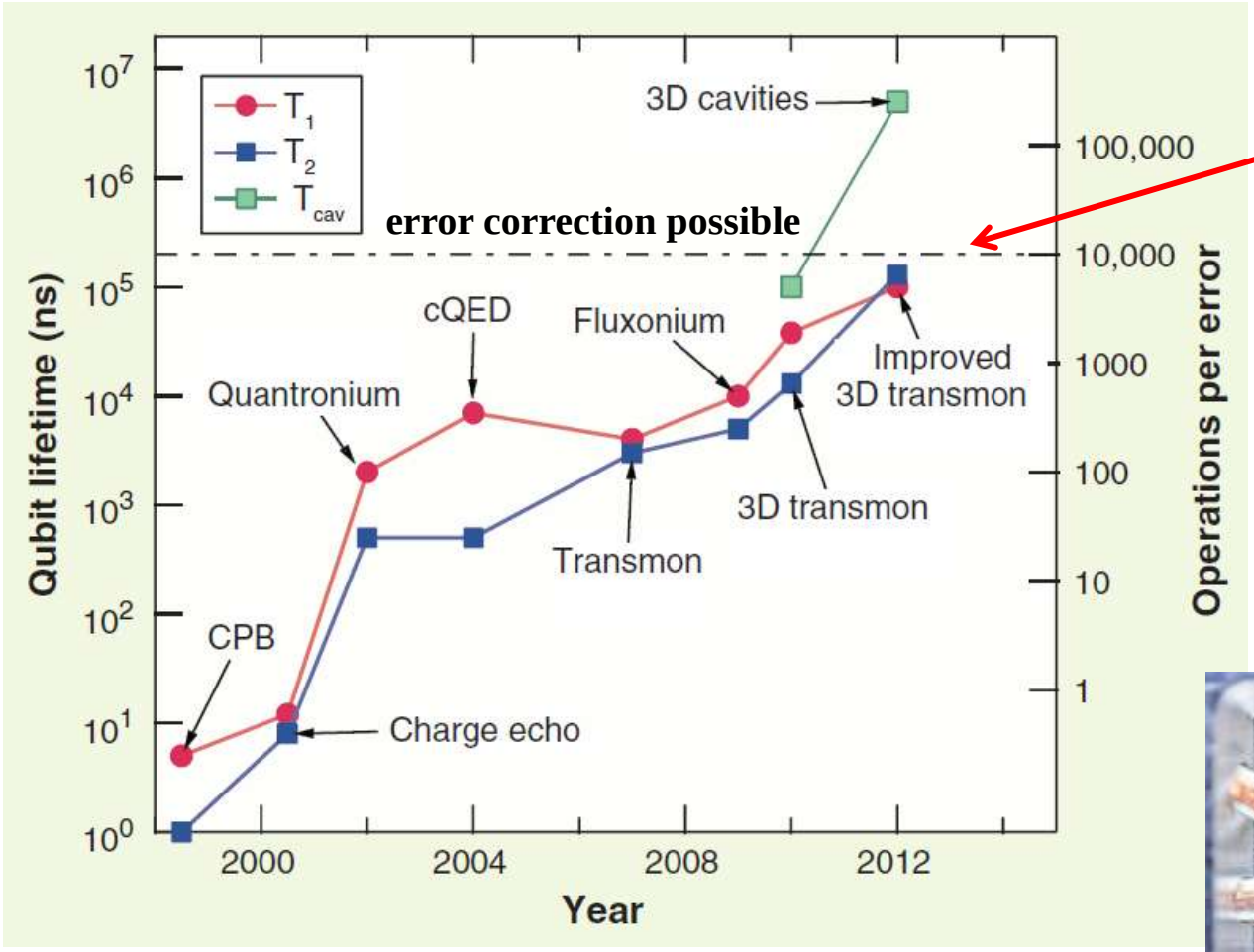

!!

Level important for quantum error correction

Modern SC qubit

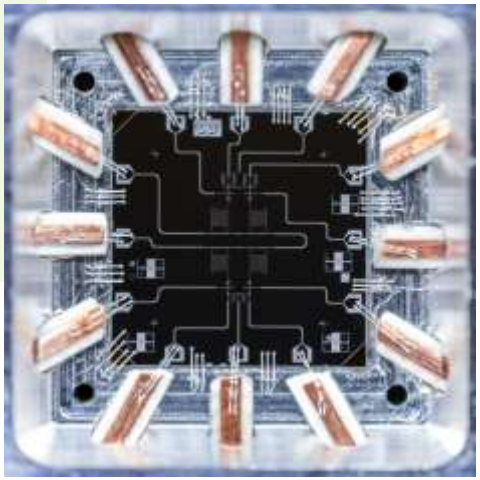

M. H. Devoret and R. J. Schoelkopf, *Science* 339, 1169 (2013)

Fabrication of SC qubits in Russia

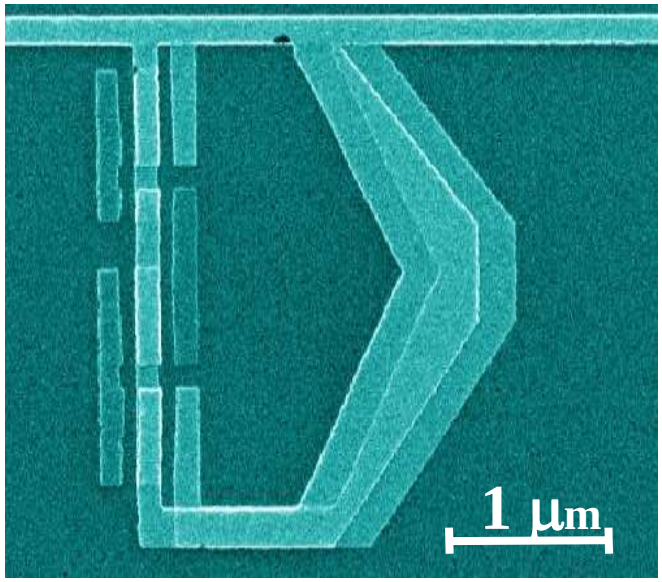

May 2015.
First qubits fabricated in Russia

Qubit Spectrum

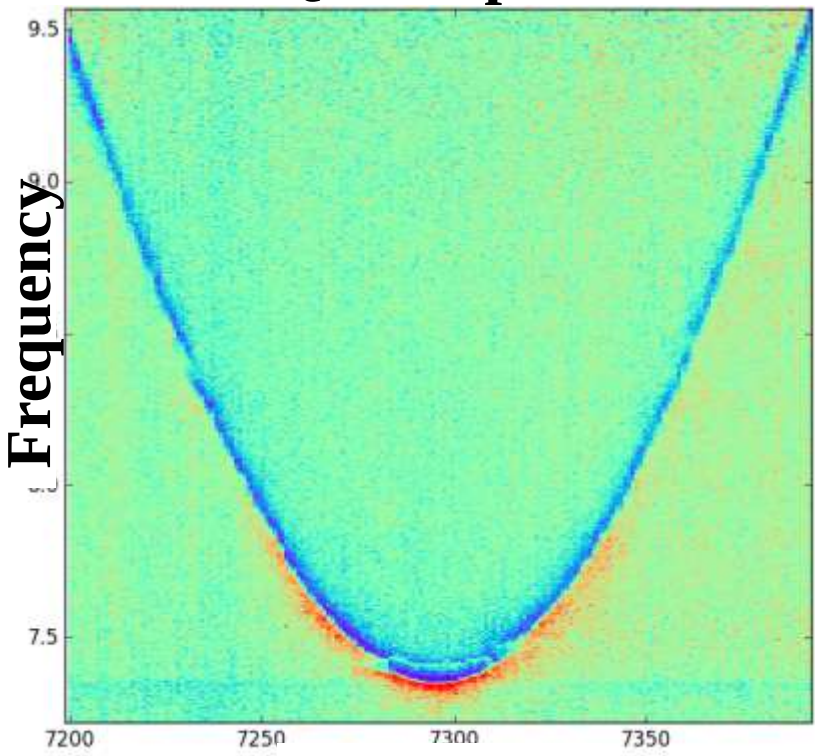

Oleg Astafiev

МФТИ
RQC
Russian Quantum Center
ИФТТ РАН
ISSP RAS

Valeriy Ryazanov

Observed Rabi oscillations

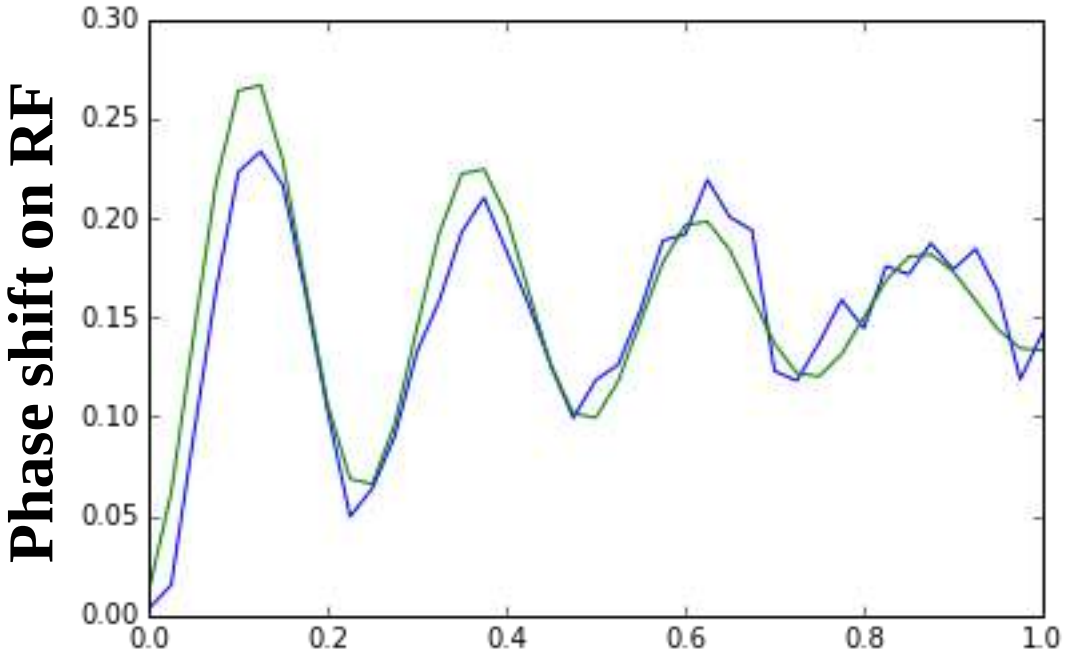

Only $5 \ll 10^4$ Rabi oscillations are observed

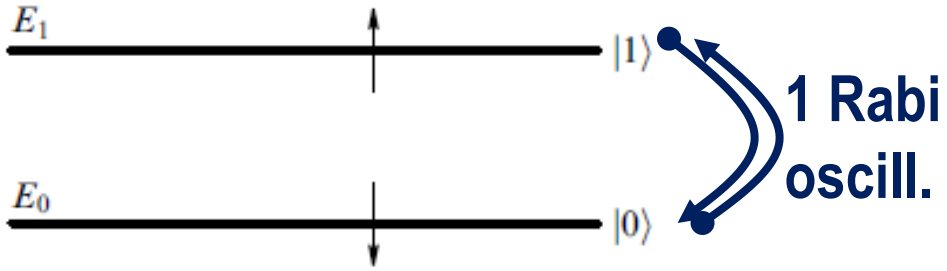

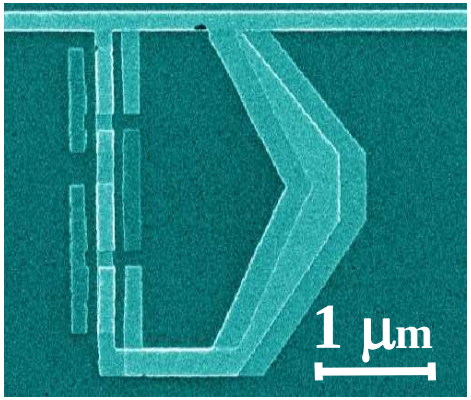

$T_1 = 525$ ns

«Modern» transmon: $T_1 \sim 20$ μs

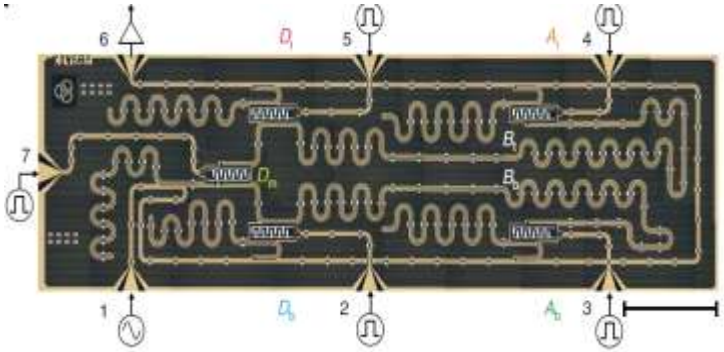

Electrons on the liquid helium surface
(general introduction).

Properties of electrons on the helium surface:

1. **Electrons float on the surface** (an electron in the bulk of helium form a bubble of energy +0.1eV)

2. **Surface electrons interact only with helium vapor and ripplons.** The system is very pure. All outer particles go out from liquid helium.

[The surfons (surface He atomic levels) are excitations with gap ~2K. They weakly interact with surface electrons (because of small wave function) and disappear at low temperature.]

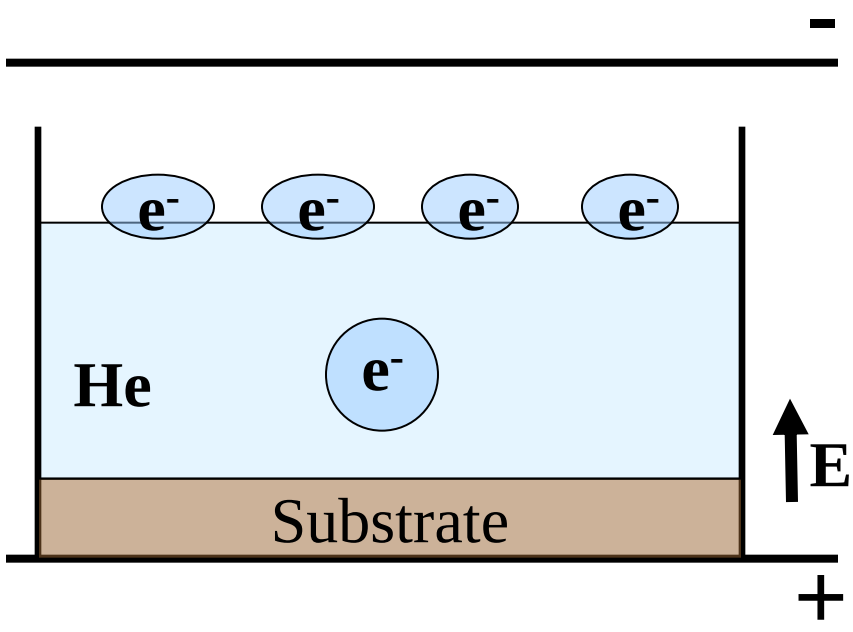

3. **Electrons on the surface may form a Wigner crystal** due to Coulomb repulsion **(first observation of 2D electron Wigner crystal)**

Electron energy as a function of height near the liquid helium surface

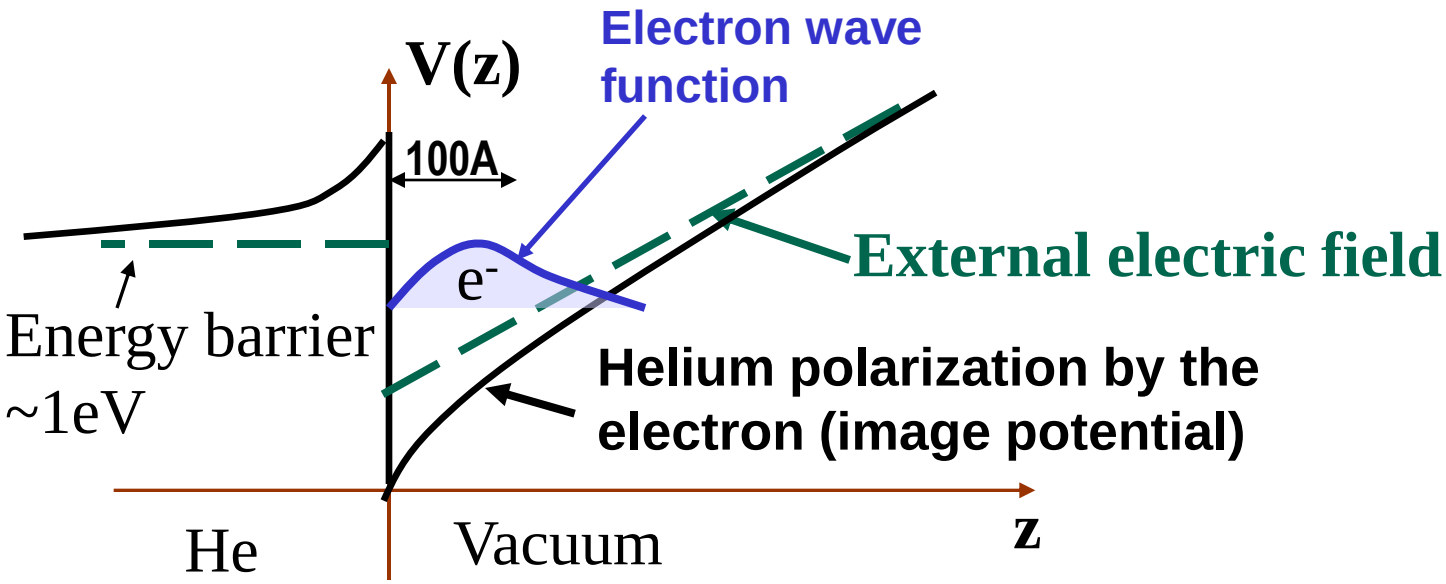

Electrons are clamped to the surface by external electric field and by image forces.

A 2D electron gas is formed on the helium surface

Maximal electron density on the liquid helium surface

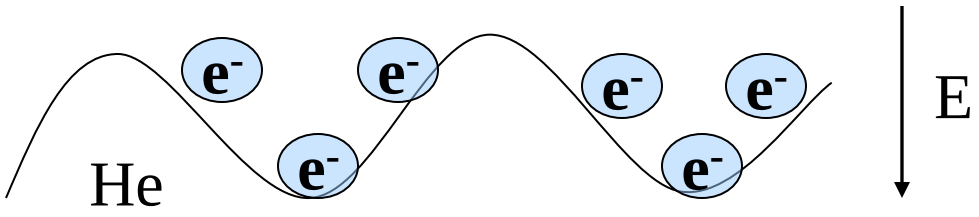

Above some critical density the charged helium surface becomes unstable.

For thick helium film the maximal areal density $n_{max} \approx 10^9$ cm^{-2}

For thing helium film maximal electron density $n_{max} \approx 10^{11}$ cm^{-2}

This is the main obstacle to create a degenerate 2D electron gas on liquid helium surface. However, it is not an obstacle for the design of one-electron devices, including SET and qubits.

Atoms on the surface quantum level (surfons)

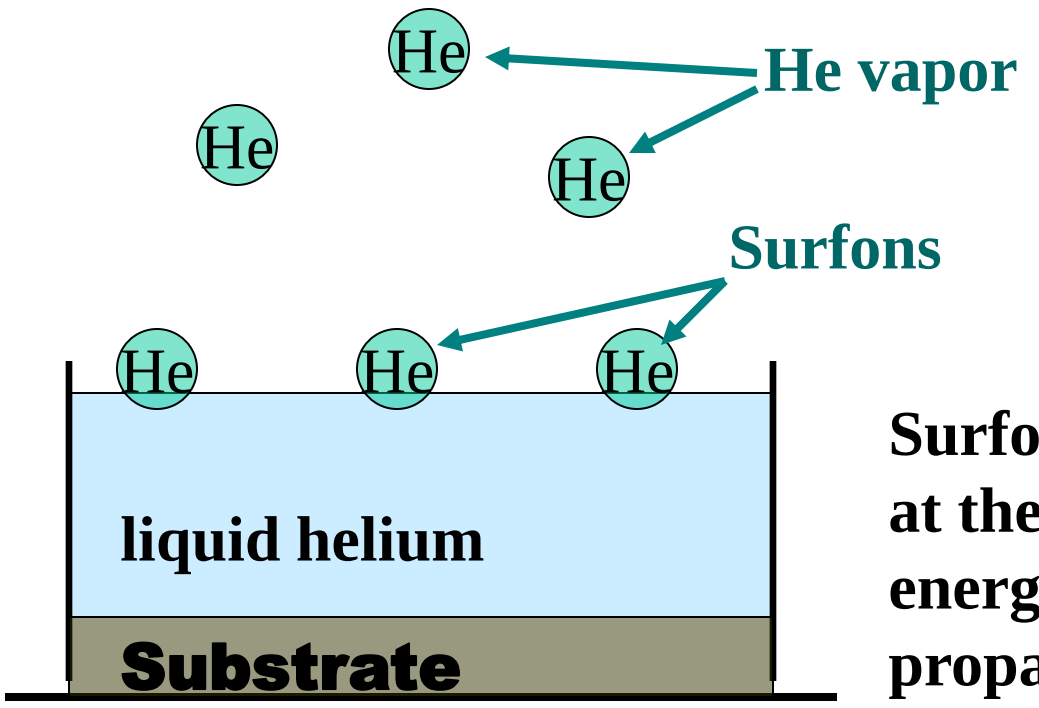

Temperature dependence of the surface tension $\Delta\sigma(T)$ of both He isotopes can be explained if we introduce a new type of excitations – surfons.

Surfon is a bound state of an atom at the surface, which has lower energy than He vapor and can propagate along the surface

Surfons interact with surface electrons. On He this interaction is weak because of small overlap of electron and surfon wave functions. However, above solid hydrogen this interaction explains the shift and width of electron transitions.

A.M. Dyugaev and P.D. Grigoriev, JETP Lett.78, 466 (2003).
A.D. Grigoriev, P.D. Grigoriev, A.M. Dyugaev, J. Low Temp. Phys. 163, 131–147 (2011)
P.D. Grigor'ev, A.M. Dyugaev, E.V. Lebedeva, JETP Lett. 87, 106 (2008); JETP 104, 1, (08)

Electrons on the liquid helium surface as quantum computing system

P.M. Platzman, M.I. Dykman, Science 284, 1967 (1999).

Quantum Computing with Electrons Floating on Liquid Helium

P. M. Platzman[1]* and M. I. Dykman[2]

A quasi–two-dimensional set of electrons ($1 < N < 10^9$) in vacuum, trapped in one-dimensional hydrogenic levels above a micrometer-thick film of liquid helium, is proposed as an easily manipulated strongly interacting set of quantum bits. Individual electrons are laterally confined by micrometer-sized metal pads below the helium. Information is stored in the lowest hydrogenic levels. With electric fields, at temperatures of 10^{-2} kelvin, changes in the wave function can be made in nanoseconds. Wave function coherence times are 0.1 millisecond. The wave function is read out with an inverted dc voltage, which releases excited electrons from the surface.

Electrons on the liquid helium surface as qubits

To be applicable as a quantum bit the system must

- **Have long relaxation time**
- **Can be controlled with high precision.**

Both these requirements can be fulfilled (in principle)
with electrons on the liquid helium surface, since
a). This system is very pure (~10^5 Rabi oscillations are feasible)
b). It allows good control via electrodes on the substrate or above He
c). Unprecedented transport efficiency for single electrons on He allows the controlled interaction between remote qubits.

As a two-level system (qubit) one can use discrete electron quantum levels (***charge*** qubit): ***vertical*** (perpendicular to the He surface) or ***horizontal***, or electron spin (***spin*** qubit).

Vertical electron levels above liquid He as qubits.

[P.M. Platzman, M.I. Dykman, Science 284, 1967 (1999)]

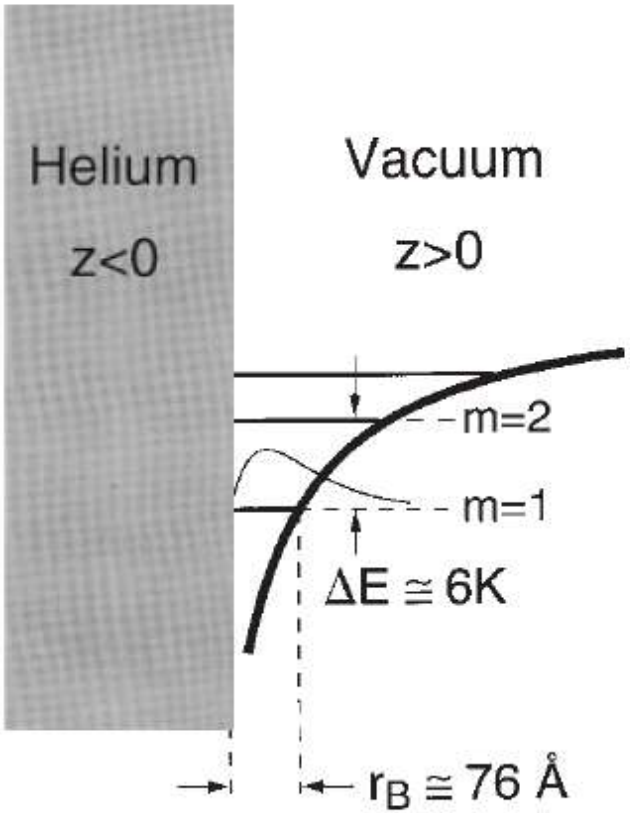

Fig. 1. The geometry for an electron trapped at the helium vacuum interface. The Rydberg energy levels along with a typical $m = 1$ wave function are displayed in the image potential $V(z) = -\Lambda e^2/z$ for $z > 0$.

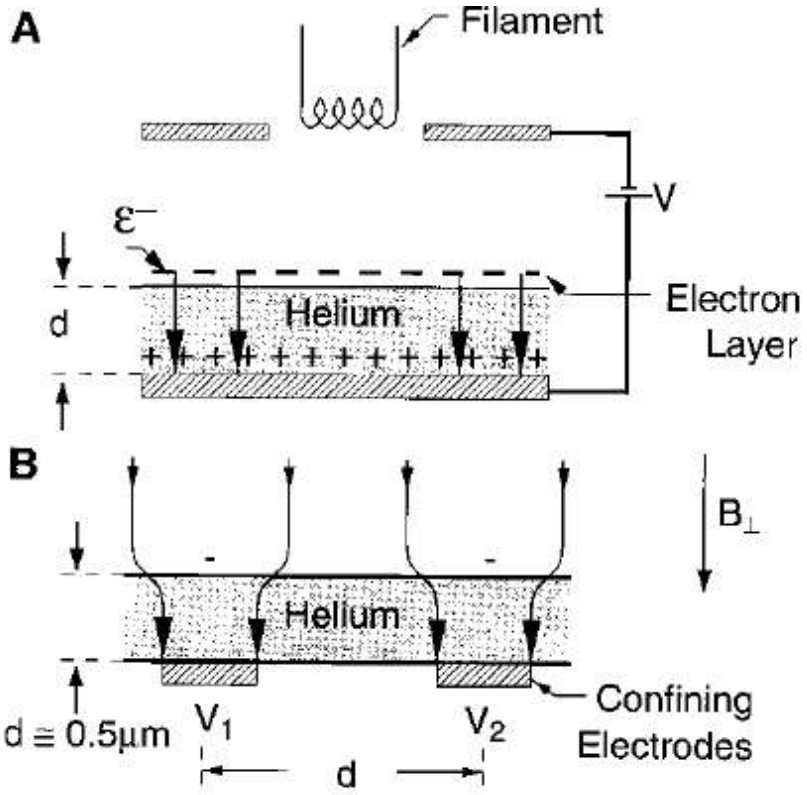

Fig. 2. (**A**) The parallel plate capacitor arrangement for confining a uniform layer of electrons. The holding field $\mathscr{E}_-$ and the filament for charging are shown. (**B**) The geometry for a pair of electrons on a patterned substrate. The rough dimensions, the shape of the field lines, and the control gate are included.

Vertical levels of surface electron for qubit: read-out configuration is very simple.

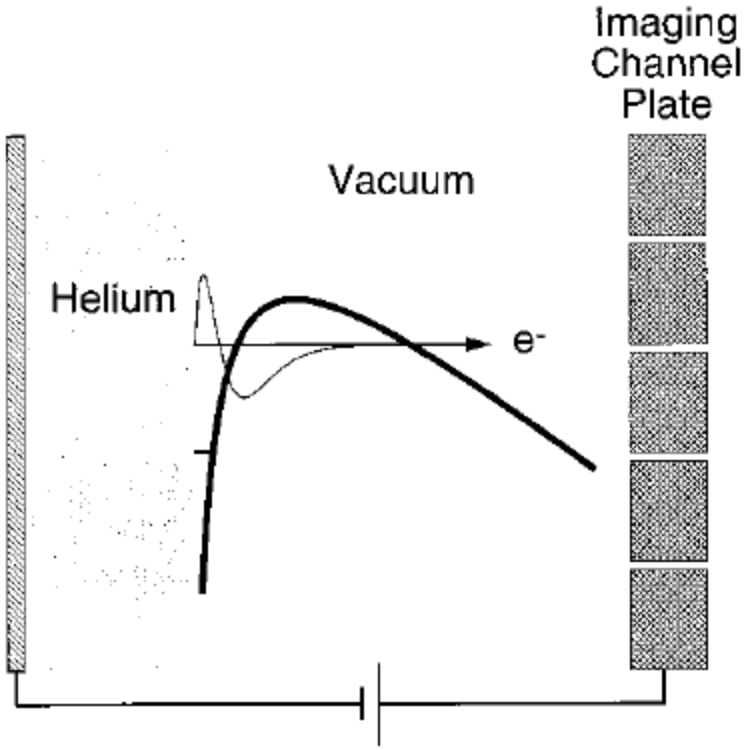

Fig. 3. The read-out configuration. The potential leading to tunneling when a reverse field is shown, along with a schematic of the position-sensitive channel plate.

Some advantages:

1). All electrons are in the same potential. They have exactly the same energy level separation if the helium film is thick.

(However, the electrodes on the substrate, confining the electrons, create some dispersion of energy levels, which depends on the electrode shape accuracy and substrate flatness.)

2). The read-out configuration is possible and quite simple.

P.M. Platzman, M.I. Dykman, Science 284, 1967 (1999)

Dephasing (dissipation) mechanisms

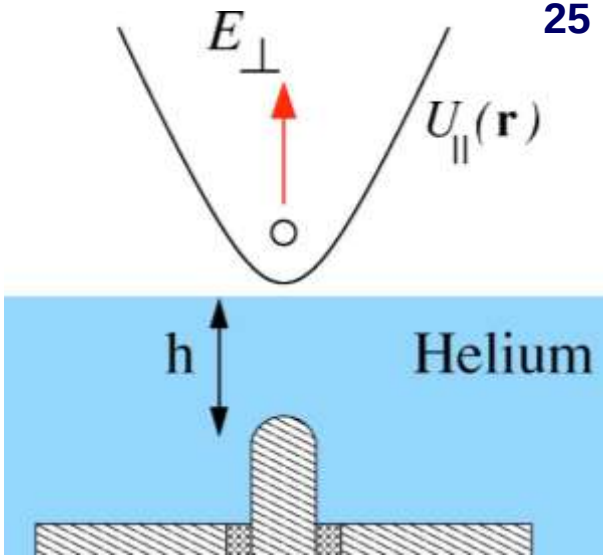

1). Interaction with surface waves (ripplons) depends on the in-plane confining potential.

a). One-ripplon decay for localized electrons is ≈0 (damped due to energy-momentum conservation laws).

b). Two-ripplon decay has small amplitude because of weak electron-ripplon interaction: $\Gamma < 5\bullet10^3\ s^{-1}$ (for $E_\perp$=300V/cm).

c). Ripplon-induced sideband absorption (electron transitions with emission or absorption of a ripplon). Loss given by Debye-Waller factor e^{-W}, W≈0.05.

2). Interaction with bulk phonons in helium (important mainly for the vertical electron transition). (a) Due to surface displacement $\Gamma < 7\bullet10^3\ s^{-1}$

(b) Due to modulation of He dielectric constant $\Gamma < 6\bullet10^4\ s^{-1}$.

3). Thermal dephasing: $\Gamma \propto T^3$; $\Gamma(T=10mK) \approx 100\ s^{-1}$.

4). Electrode noise: (a). Electric noise in the electrode at *T=1K*, $\Gamma \sim 10^4\ s^{-1}$.

b). Variations of shape and size gives energy-level variation for different qubits.

[M.I. Dykman, P.M. Platzman, P. Seddighrad, PRB 67, 155402 (2003)].

Localized electron state on the helium surface: horizontal energy levels are also useful for qubits

1.) Positively charged electrode or impurity on the substrate confines the electrons along the surface and creates a very pure quantum dot.

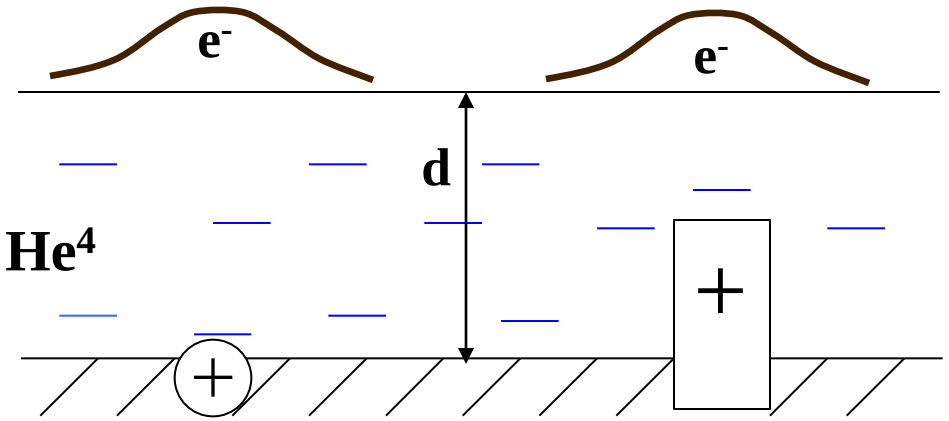

In-plane impurity or electrode potential for surface electrons:

$$V(r) = \frac{-e^2}{\sqrt{r^2 + h^2}}$$

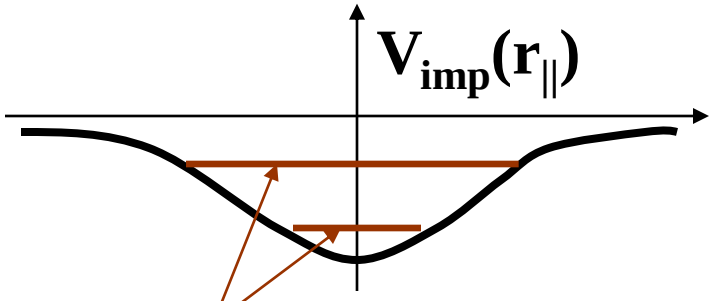

Lowest energy levels are separated by **Δ ~ 4K**

2). External magnetic field also confines the electrons.

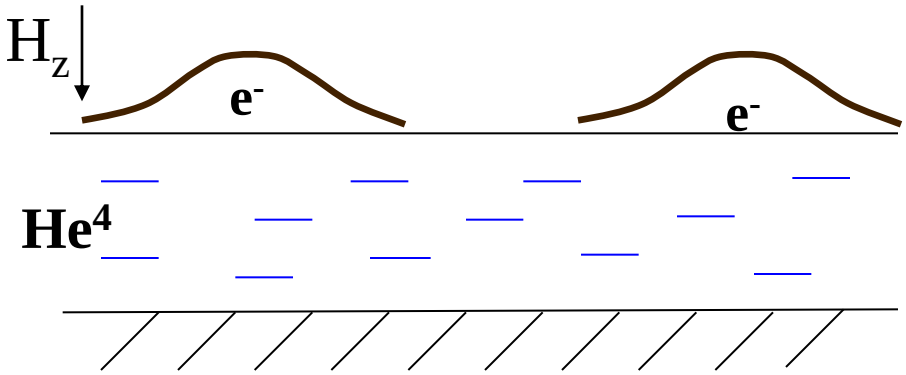

One-ripplon electron transitions are exponentially damped => long decoherence time.

Calculation of energy levels, and line width and shape for transitions between localized electron states.

P. D. Grigor'ev, JETP Lett. 66, 630 (1997)
P. D. Grigor'ev and A. M. Dyugaev, JETP 93, 103 (2001)

At low temperature surface electrons have inelastic scattering only by ripplons (surface waves)

To consider the electron-ripplon interaction for localized electrons one can apply the exactly solvable **independent boson model**, because the one-ripplon transitions have exponentially small matrix element

(the perturbation theory and the path integral approach in quasiclassical approximation cannot give an accurate answer).

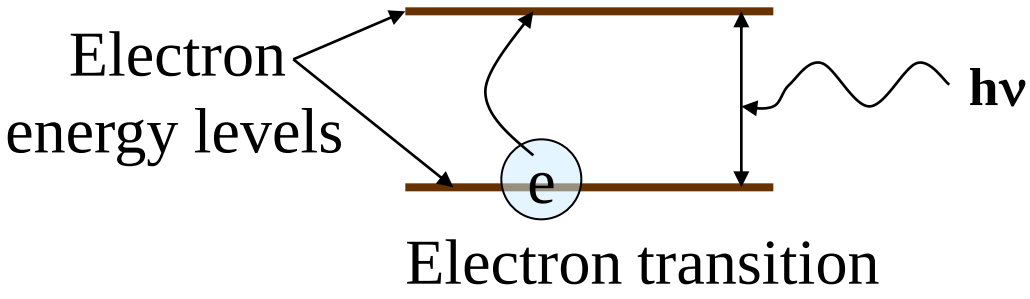

Line shape and width I(ω) -?

Physical origin of the optical absorption line broadening (sideband effect)

Surface deformation (ripplonic polaron) under an electron in different states is different → **The electron transition is accompanied by relaxation of a dimple under an electron**

This relaxation leads to the transition line broadening. The shape of absorption line depends on the ratio between the dimple relaxation time and electron transition time. In general case, it may have two maxima:

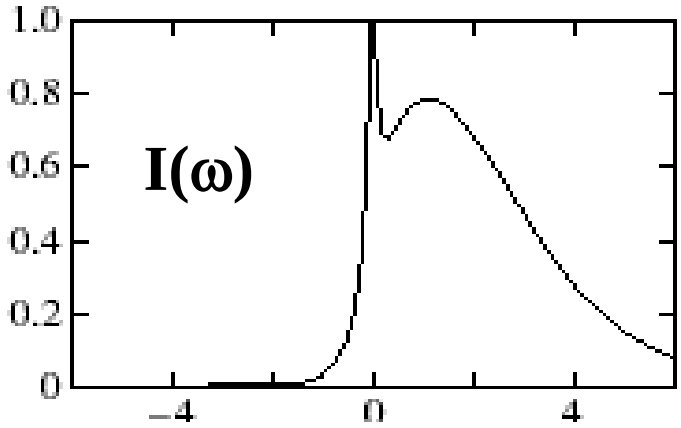

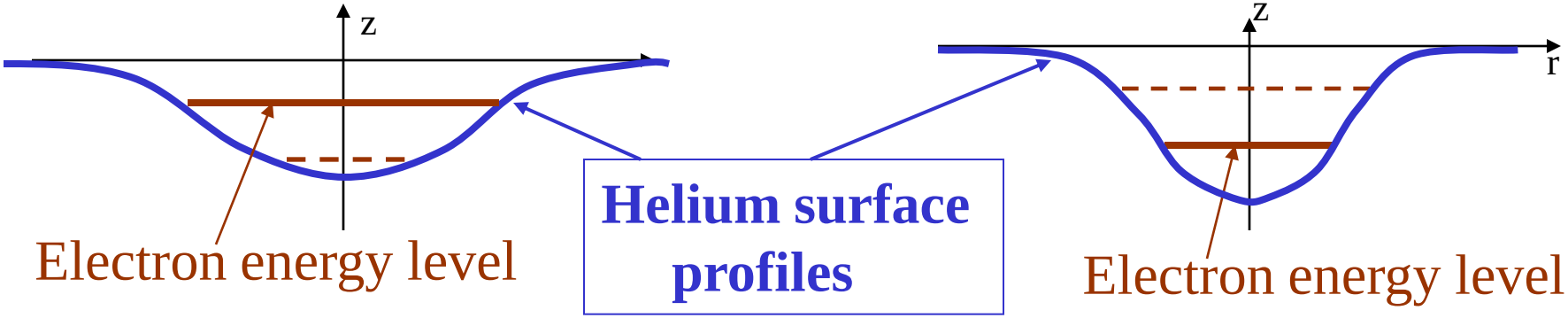

[P. D. Grigor'ev and A. M. Dyugaev, JETP 93, 103 (2001)]

The model.

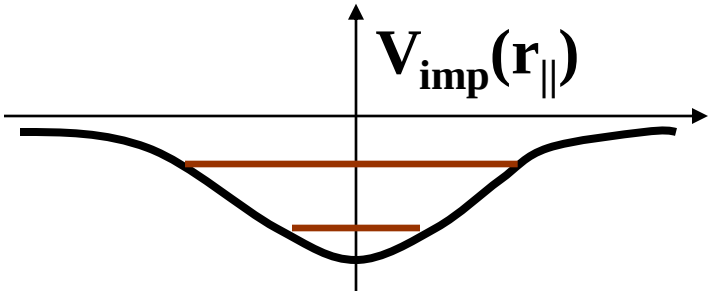

Hamiltonian (of independent boson model)

$$\hat{H} = \sum_i \varepsilon_i C_i^+ C_i + \sum_q \hbar\omega_q a_q^+ a_q + \sum_{i,q} M_{i,q}(a_q^+ + a_q) C_i^+ C_i$$

Ripplon dispersion $\omega_q^2 = \frac{\alpha_{He}}{\rho_{He}} q(q^2 + \kappa^2) \tanh qd$,

where $\kappa = 20 cm^{-1} << q, \quad \alpha_{He4} = 0.36 dyn/cm, \quad \rho_{He4} = 0.147 g/cm^3.$

The matrix element of the electron-ripplon interaction

$$M_{i,q} = \int d^2\mathbf{r} \, |\Psi_i|^2 \, e^{i\mathbf{qr}} Q(q) F(q), \; Q(q) \equiv \frac{\hbar q \tanh qd}{2\rho\omega_q},$$

where

$$F(q) = eF_\perp + \int_0^\infty \frac{(\varepsilon - 1)e^2 q}{4(\varepsilon + 1)z} \left(\frac{1}{qz} - K_1(qz) \right) \varphi^2(z) dz .$$

Solution of the independent boson model

The independent boson model is solved by the transformation

$$\bar{H} = e^{S} H e^{-S}, \quad \text{where} \quad S = \sum_i C_i^+ C_i \sum_q (M_{qi}/\omega_q)(a_q^+ - a_q).$$

The new Hamiltonian is diagonal:

$$\bar{H} = \sum_i (\varepsilon_i - \Delta_i) C_i^+ C_i + \sum_q \hbar\omega_q \bar{a}_q^+ \bar{a}_q .$$

The shift of energy levels $\Delta_i = \sum_q M_{qi}^2 / \hbar\omega_q .$

New ripplon operators $\bar{a}_q = a_q - \sum_i (M_{qi}/\omega_q) C_i^+ C_i .$

New electron operators

$$\bar{C}_i = C_i \exp\left\{ - \sum_q (M_{qi}/\omega_q)(a_q^+ - a_q) \right\}.$$

Calculation of light absorption line

The intensity of light absorption can be calculated using the Kubo formula:

$$\mathrm{Re}\,\sigma_{\alpha\beta}(\omega) = \frac{1}{2\omega}\int_{-\infty}^{\infty} e^{i\omega t}\left\langle j_\alpha(t)\, j_\beta(t)\right\rangle dt,$$

where the current operator $j_\alpha = \sum_{i,j} P_{ij,\alpha}\bar{C}_i^{+}\bar{C}_j.$

After calculation one obtains

$$\mathrm{Re}\,\sigma_{\alpha\beta}(\omega) = \frac{1}{2\omega}\sum_{i,j} n_i(1-n_j)P_{ij,\alpha}P_{ij,\beta}\int_{-\infty}^{\infty}\exp\left\{it(\omega+\varepsilon_i-\varepsilon_j-\Delta_i+\Delta_j)-\Phi_{ij}(t)\right\}dt,$$

where

$$\Phi_{ij}(t) = \sum_q \frac{(M_{qi}-M_{qj})^2}{\omega_q^2}\left[(n_q+1)(1-e^{-i\omega_q t})+n_q(1-e^{i\omega_q t})\right].$$

There are 3 energy parameters in the problem: (1) Ripplon energy ω_a; (2) Temperature T; (3) Energy of surface deformation Δ

Or there are 2 dimensionless parameters: $T_* = T/\omega_a$ and $A = \Delta/\hbar\omega_a$

Results I (high temperature limit T*>>1)

a). Strong coupling limit

$$\nu \equiv AT_* > 1 (A \equiv \Delta / \hbar\omega_a).$$

Absorption line has Gaussian shape

$$I(\omega_*) \sim \exp\left\{-\frac{(\omega_* - A)^2}{4AT_*}\right\}, \omega_* \equiv \frac{\omega - \omega_0}{\omega_a}.$$

b). Weak coupling limit $\nu \equiv AT_* < 1.$

$$I(\omega_*) = I(0)\left(1 - \frac{\omega_*^2}{4(\nu - 3/2)}\right), \omega_* << 1;$$

$$I(\omega_*) \propto \exp\left(-|\omega_*|\right)|\omega_*|^{\nu-1}, |\omega_*| << 1.$$

Urbah rule (the temperature independent exponential tails of absorption line) has been observed in many solid-state systems This is its first theoretical substantiation.

P.D. Grigor'ev, A.M. Dyugaev, JETP 93, 103 (2001)

The crossover from Gaussian to exponential tails as the coupling energy reduces is clearly seen.

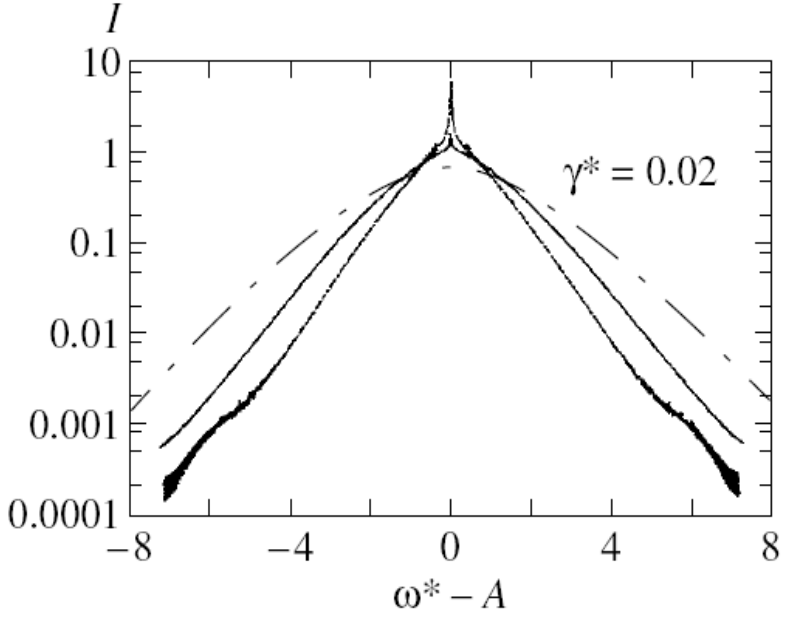

Fig. 2. The intensity of absorption on a logarithmic scale as a function of reduced frequency $\omega^* \equiv (\omega - \omega_0 - \Delta)/\omega(a)$. At a constant temperature $T^* = 100$, the coupling constant varies. The solid line corresponds to $\nu = 1$ ($A = 0.01$), the dot-and-dash line corresponds to $\nu = 2$, and the dotted line corresponds to $\nu = 0.5$ ($A = 0.005$). For a low value of ν, one can clearly see the linear portions of the dependence $\ln I(\omega^*)$ (Urbach rule, Eq. (34)). If $\nu < 1$, a sharp peak at $\omega^* = 0$ is also observed.

Results II (low temperature limit T*<< 1)

a). Strong coupling limit $A \equiv \Delta / \omega_a >> 1$ where $\Delta = F^2/32\alpha \sim 0.01K.$ is the energy of surface deformation due to dimple, and typical ripplon energy $\omega_a \sim 0.01K$.

Absorption line has Gaussian shape

$$I(\omega_*) \propto \exp\left\{-\frac{(\omega_* - A)^2}{4A}\right\}, \quad \omega_* \equiv \frac{\omega - \omega_0}{\omega_a}.$$

b). Weak coupling limit $A << 1$. $T_* \equiv T / \omega_a$

$$I(\omega_*) \propto A\left[\frac{T_*}{|\omega_*|}\exp\left(-\frac{|\omega_*|}{T_*}\right) + e^{-\omega_*}\theta(\omega_*)\right].$$

The singularity at $\omega_* = 0$ reflects the very narrow absorption line within this model. This limit is the most interesting for quantum computation applications.

c). In the intermediate case $A \sim 1$ absorption line has maxima: the thing adiabatic peak which survives as A reduces and the thicker quick-time non-adiabatic maximum at $\omega_* \sim A$.

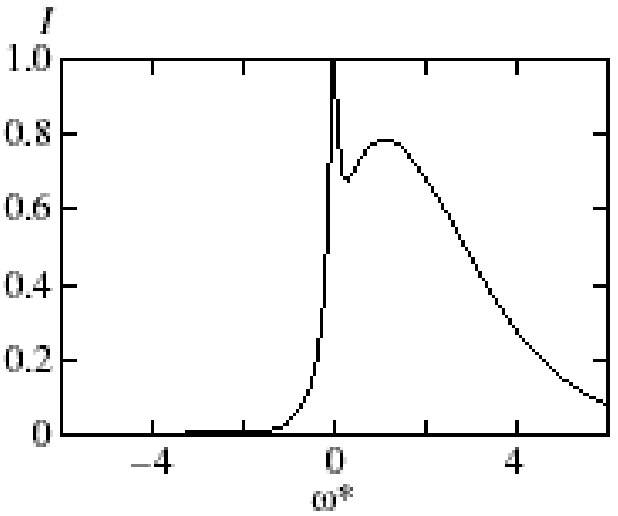

Conclusion: the horizontal electron levels are also suitable for qubits.

P.D. Grigor'ev, A.M. Dyugaev, JETP 93, 103 (2001)

Spin qubits with electrons on He surface

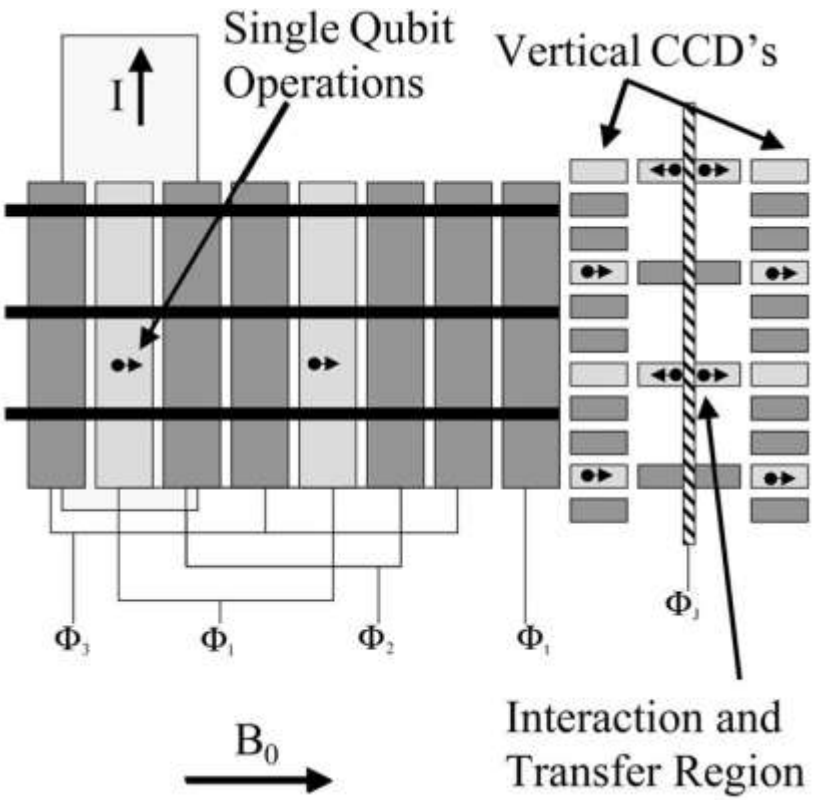

S. A. Lyon, PRA 74, 052338 (2006)

FIG. 1. A schematic diagram of a possible gate electrode arrangement for a quantum computer. The grey regions are conducting gates held at different potentials arranged as a three phase CCD. By adjusting the gate voltages Φ_j , the electrons dots with arrows can be moved around the device. The light-colored region on the left represents a conductor below the gates through which a current *I* can be run, producing a local lateral magnetic field that combines with the large constant field, B_0, *to bring the Zeeman* transition of the electrons above the wire into resonance with applied microwaves.

Advantages:

(1) very low error rate: coherence time >100s, very high electron transmission efficiency
(2) easy initial-state control: start with ground state in B and apply fixed-time rf power.
(3) Possible readout, e.g. by compare the unknown spin with a known one.
(4) Possible control of qubit interaction (!): exchange (by controlled distance) or dipole.

Control of interaction between electron spins on He surface

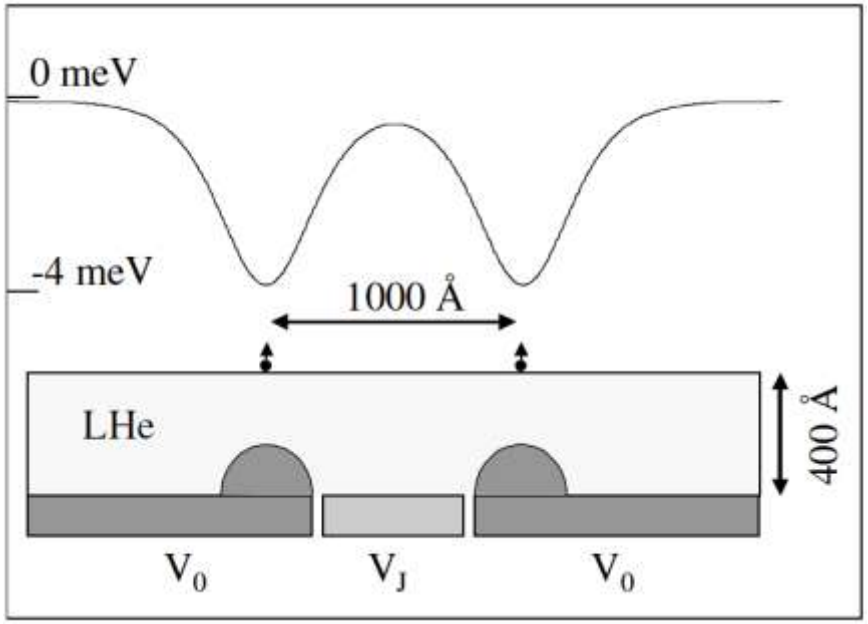

Fig: the overlap of wave functions of two electrons (dots with arrows) is controlled by changing the gate voltage V_J, allowing controllable exchange or magnetic-dipole interaction between electron spins.

The dipole-dipole magnetic interaction

$$H_D = \frac{\mathbf{u}_1 \cdot \mathbf{u}_2}{r^3} - \frac{3(\mathbf{u}_1 \cdot \mathbf{r})(\mathbf{u}_2 \cdot \mathbf{r})}{r^5}$$

between two spins is sufficient for CNOT:

$$\mathrm{CNOT} = R_{1y}(-\pi/2) P R_{1y}(\pi/2)$$ where

$$P = \frac{R_{2z}(\pi/2) V_D(\pi/2) R_{1z}(\pi/2) R_{2z}(-\pi/2) V_D(\pi/2) R_{2z}(\pi/2)}{\sqrt{i}}$$

$$= \begin{pmatrix} 1 & 0 & 0 & 0 \\ 0 & 1 & 0 & 0 \\ 0 & 0 & 1 & 0 \\ 0 & 0 & 0 & -1 \end{pmatrix}$$ produces a phase gate

$R_{xi}(\phi)$ is a rotation of spin x by angle ϕ about axis i, and turning on the dipole interaction for a time τ is

$V_D(\Phi)$ where $\Phi = \frac{\mu_0}{4\pi} \frac{g^2 \mu_B^2}{r^3} \frac{\tau}{\hbar}$

Conclusion: all necessary steps for quantum computing with electron spin qubit on He surface are feasible [S. A. Lyon, PRA 74, 052338 (2006)]

Proposal for Manipulating and Detecting Spin and Orbital States of Trapped Electrons on Helium Using Cavity Quantum Electrodynamics

D. I. Schuster,[1] A. Fragner,[1] M. I. Dykman,[2] S. A. Lyon,[3] and R. J. Schoelkopf[1]

We propose a hybrid architecture in which an on-chip high finesse superconducting cavity is coupled to the lateral motion and spin state of a single electron trapped on the surface of superfluid helium. We estimate the motional coherence times to exceed 15 μs, while energy will be coherently exchanged with the cavity photons in less than 10 ns for charge states and faster than 1 μs for spin states, making the system attractive for quantum information processing and strong coupling cavity quantum electrodynamics experiments. The cavity is used for nondestructive readout and as a quantum bus mediating interactions between distant electrons or an electron and a superconducting qubit.

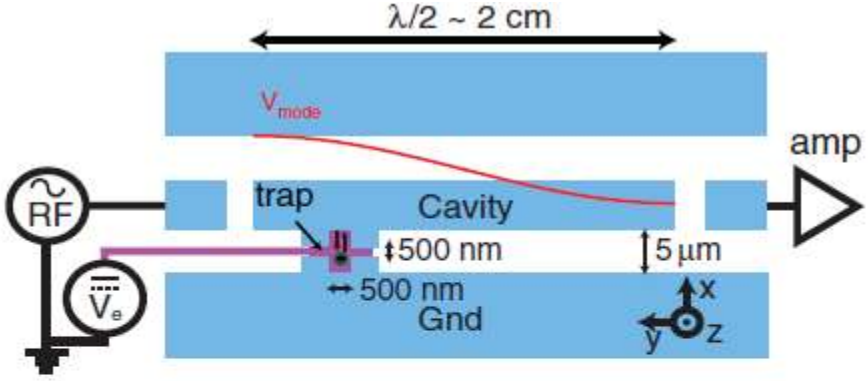

FIG. 1 (color). Top view of electrostatic electron trap. The ground plane and cavity center pin are shown in blue, while the trap electrode is magenta. The configuration of center pin and ground plane provide two-dimensional confinement. A dc voltage, V_e is provided via a wire insulated from the resonator. Manipulation and readout is performed via a radio frequency voltage applied to the input port of the resonator with the modified signal measured by a cryogenic amplifier at the output port.

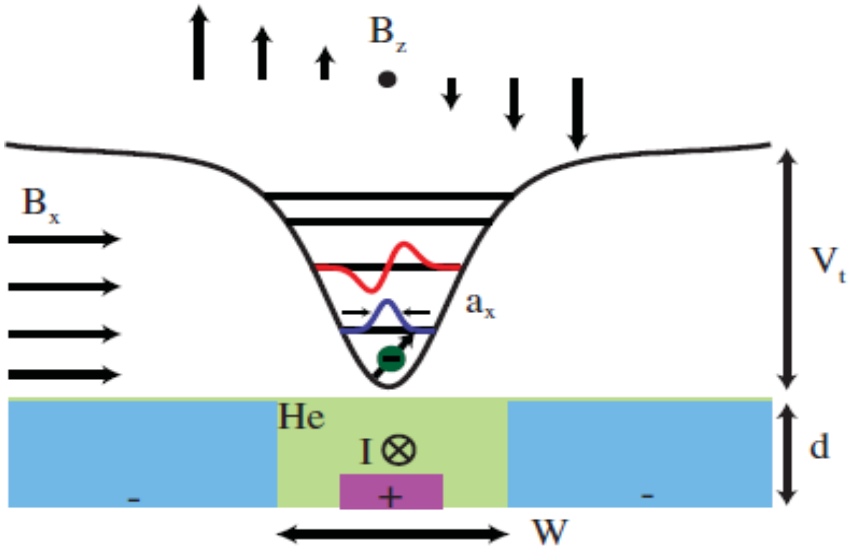

To couple the motional and spin degrees of freedom a current is sent through the center electrode creating z-field gradient in the trap

What about ^{3}He impurities on the ^{4}He surface?

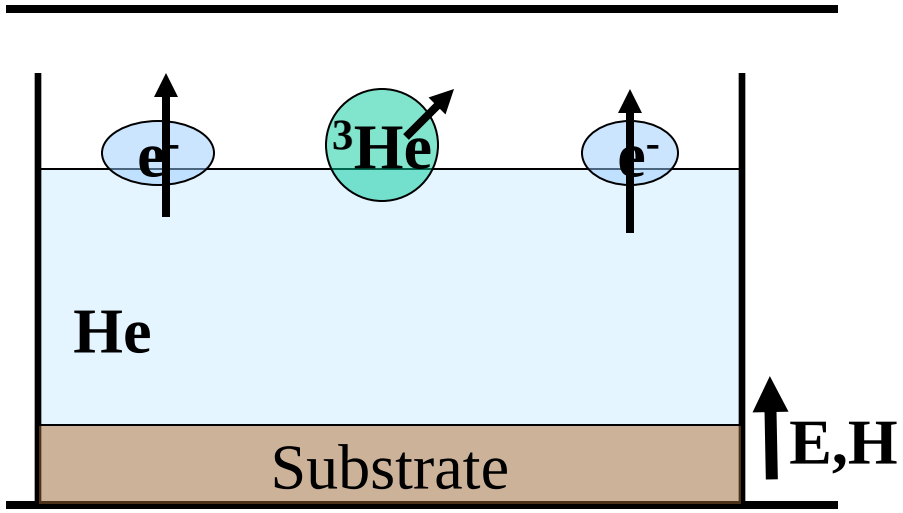

Answer: ^{3}He impurities can be completely! removed from ^{4}He surface by a cold neutron beam. This requires a neutron source or prepared (by neutrons) pure ^{4}He.

Other methods of removing ^{3}He impurities from ^{4}He surface are also possible.

Negative ions on the helium surface as qubits

[P.D. Grigor'ev, A.M. Dyugaev, JETP 88, 325 (1999)]

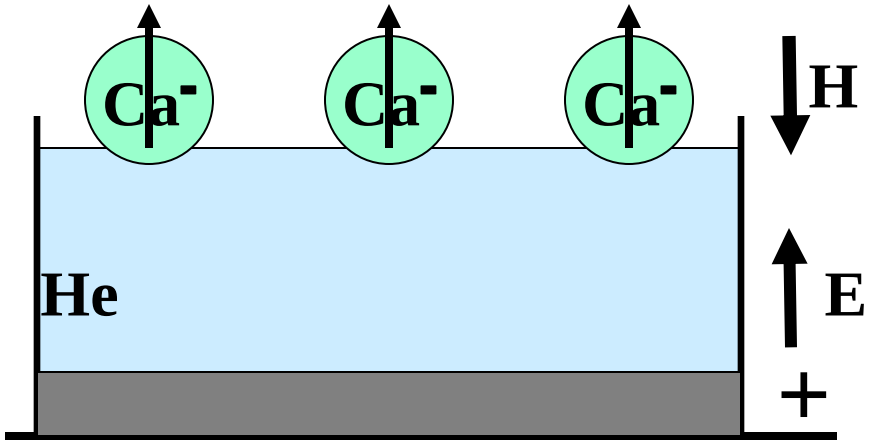

Advantages:

- They have long spin relaxation time => high coherence.
- The negative ions are strongly localized and can be easier manipulated than the electrons.
- Easier qubit interaction. Dipole interaction of Ca^- is stronger than of e^- since they can be placed much closer to each other. The interaction between Ca^- spins via e^- is possible (RKKY).

Drawbacks:

- Only spin degree of freedom has long relaxation time and can be used as a bi-level system for qubit.

Electron inside liquid helium

He

e^-

Electron in the bulk of liquid helium form a bubble of radius R_0 =18A.

The energy of this bubble is a sum of 3 terms:

$$E(R) = \frac{h^2}{2mR^2} + 4\pi\alpha R^2 - \frac{\varepsilon - 1}{2\varepsilon} 1.35 \frac{e^2}{R}$$

Quantum electron kinetic energy

Surface tension

polarization of helium

potential

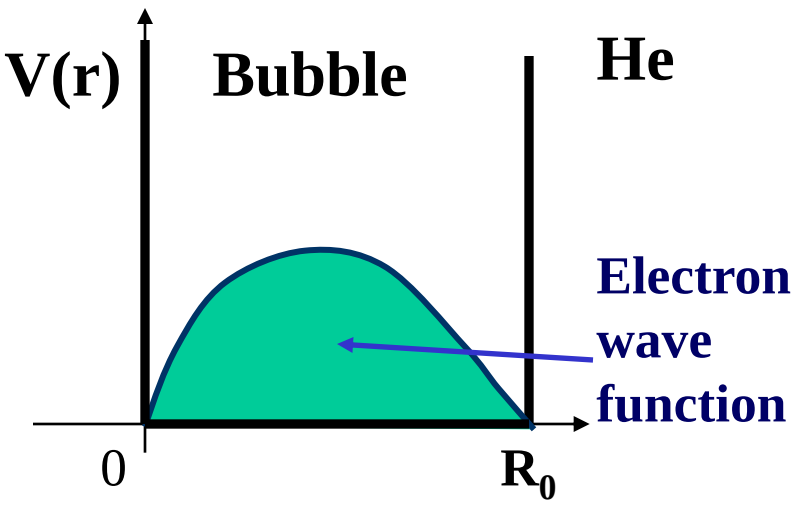

The energy loss of bubble formation is ~ 0.1eV

Calculation of ion energy in helium

The Shrödinger equation for outer electron in the effective potential is solved numerically for ion inside helium and on its surface.

Model potential for outer electron of a negative ion inside helium:

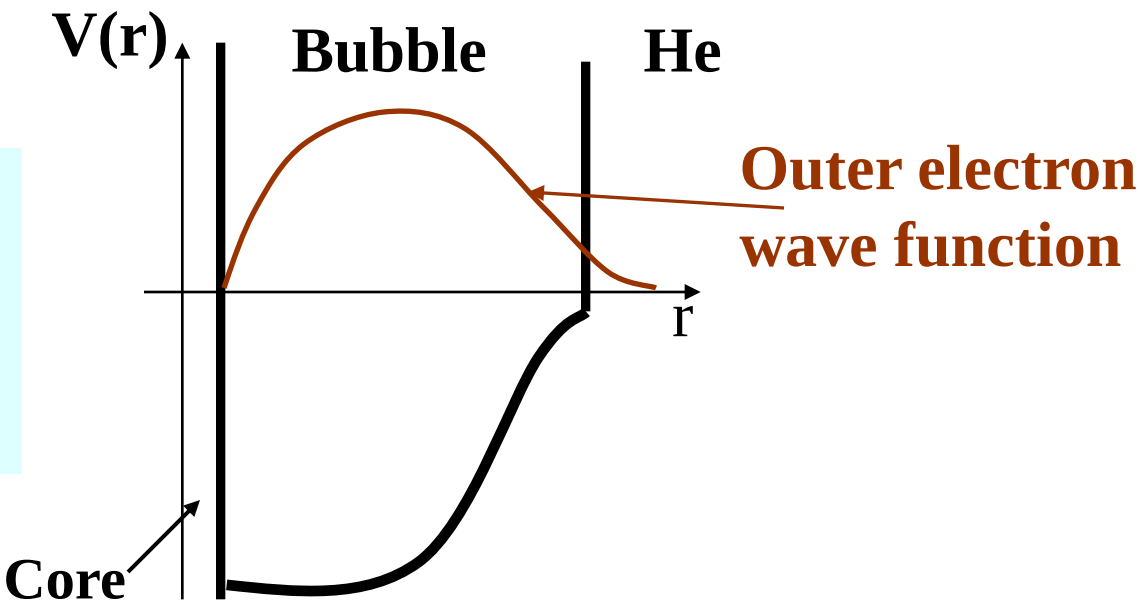

Conclusion:

Energy of Ca^- and Ba^- inside helium is higher than on its surface.

$$\Delta E_{Ba} = 0.024 eV;\ \Delta E_{Ca} = 0.006 eV.$$

Results:

TABLE I. Numerical calculations of bubble energy and optimal radius in bulk liquid helium and on its surface for several typical ions of large radius, with characteristics of these ions.

Ion	Electron affinity in vacuum E_0, eV	Ion size in vacuum $1/\kappa_0$, Å	Atom or molecule polarizability β, a_B^3	Turning point $r_0=(\alpha/a_B\kappa_0^2)^{1/4}$, Å	Optimal bubble radius in helium R, Å
O_2^-	−0.46	2.87	10.6	2.23	8.0
Ba^-	−0.145	4.87	270	6.5	12.0
Ca^-	−0.0245	11.84	170	9	14.1

Ion	Correction to ion energy in helium volume $E_{in}-E_0$, eV	Optimal separation between ion and surface h, Å (estimate)	Correction to ion energy on surface E_{sur} taking into account hole shape, eV (estimate)	Potential barrier for ion on surface of thick helium film Δ, eV
O_2^-	−0.024	–	–	≈0
Ba^-	0.024	14	−0.011	0.04
Ca^-	0.060	20	−0.003	0.065

Negative ions on the surface of liquid helium

Feature: much heavier than electrons.

Applications:

1). To observe the Wigner crystal of negative ions directly (e.g. by neutron scattering).

2). To separate the role of quantum effects in the behavior of surface electrons (e.g., quantum melting of Wigner crystal at high electron density $n_e \sim 10^{12}$ cm^{-2} etc.)

3). To create localized qubits (spin ½ in magnetic field).

4). To create new negative ions which do not exist in vacuum but exist on the helium surface or inside liquid helium (when the attraction of outer electron is close but not enough to form a bound state with atom).

5) To prove the existence of surfons (atoms on surface level).

The advantage of easy geometrical control is very important for managing qubits.

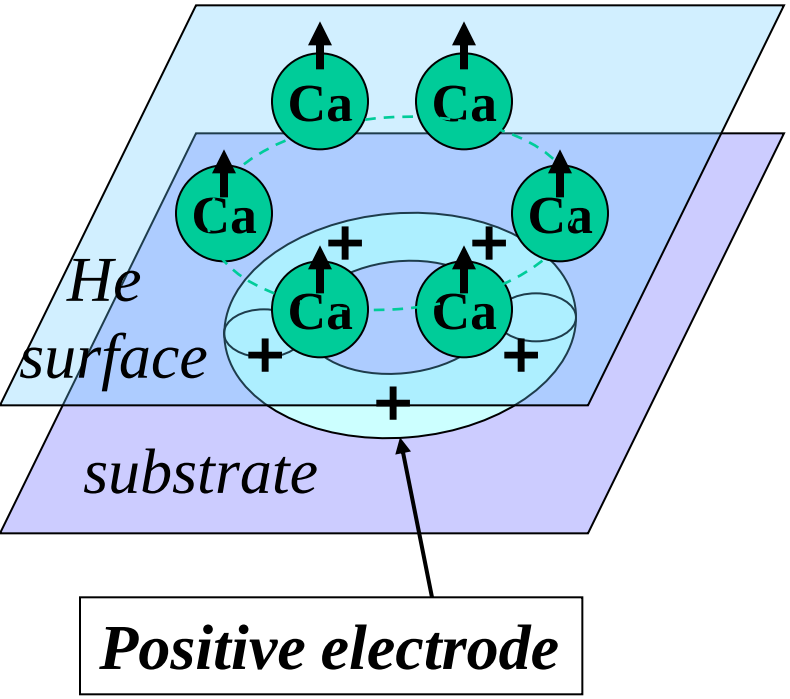

Several negative ions can be much closer to each other than electrons because there is no loss in the kinetic energy. => (1) This increases inter-qubit interaction. (2) They can be easier manipulated. (3) Interaction between ion spins can be via additional electron (not dipole-dipole) Large number of negative ions has the same limitation of density as the electrons on He surface (10^9 cm^{-2}).

[P.D. Grigor'ev, A.M. Dyugaev, JETP 88, 325 (1999)]

Part 3: Experiments with localized electron states above liquid helium

"Trapping single electrons on liquid helium", P. Glasson et al., Journal of Physics and Chemistry of Solids 66, 1539 (2005)

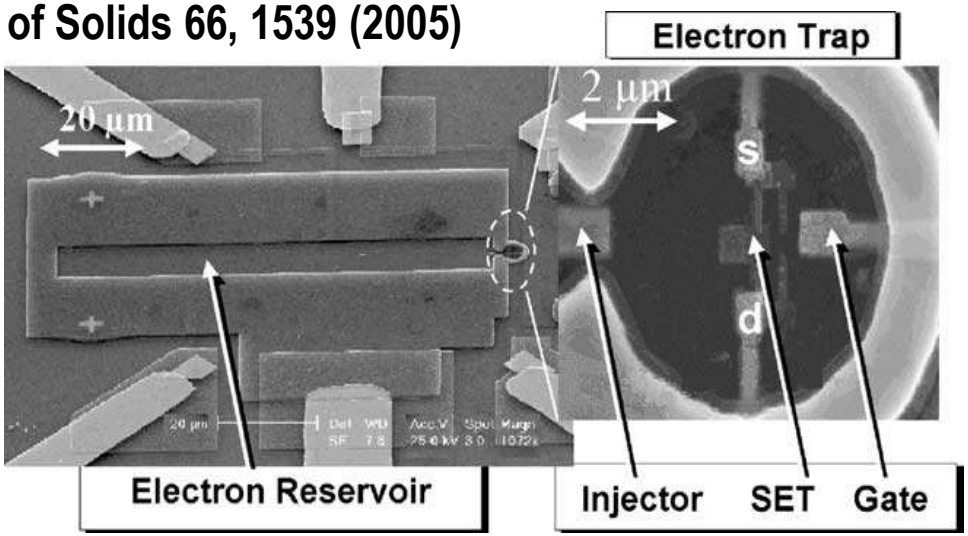

Fig.1. Microelectronic device for trapping electrons on helium surface.

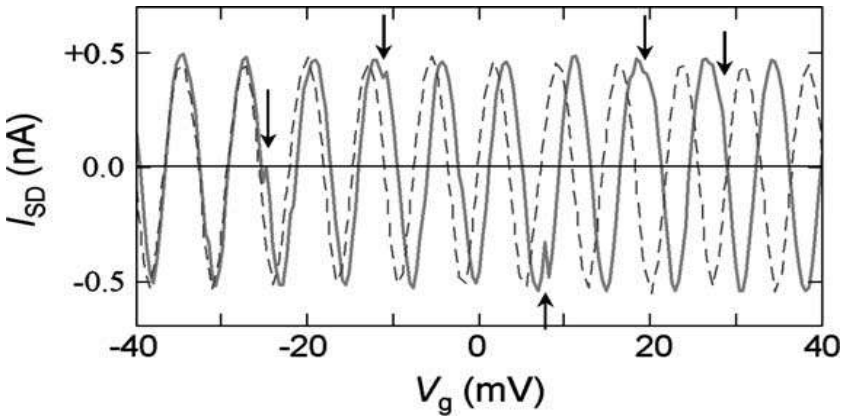

Fig. 2. Coulomb blockade oscillations by sweeping gate voltage V_g before (dotted) and after (solid) charging helium surface.

Fig. 4. Coulomb staircase for individual electrons. Charge steps (0.092 e) are seen in $\Delta Q^*/e$ as electrons leave the trap one by one until the trap is empty. The inset shows the potential profile of the trap for appropriate values of V_g.

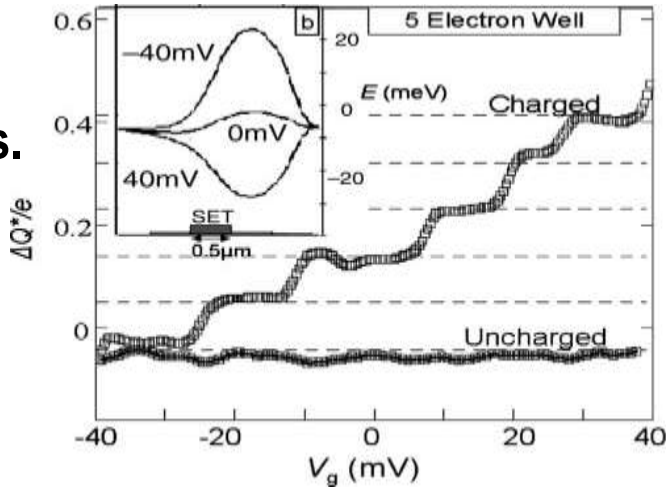

Array of 5 localized electrons above liquid helium

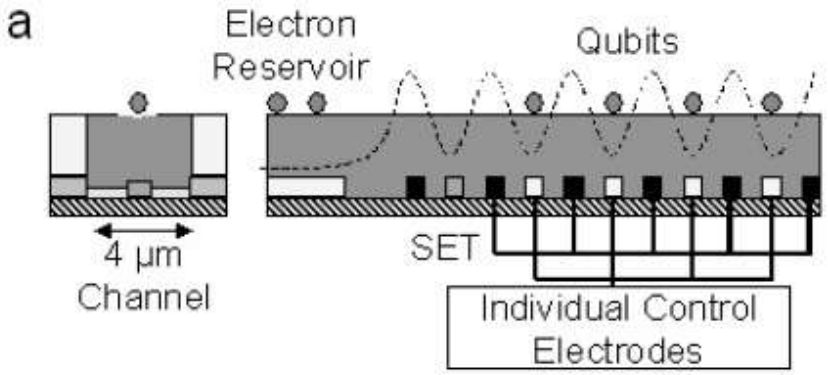

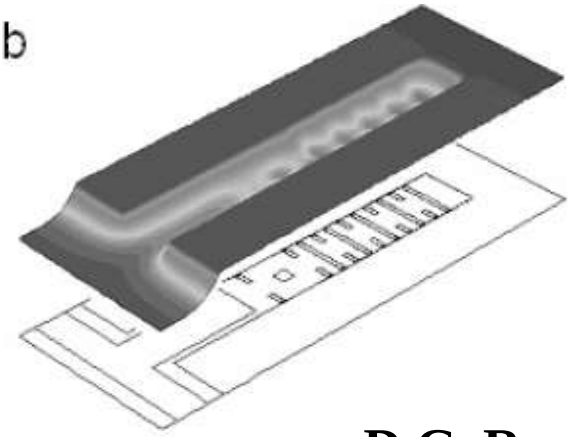

D.G. Rees et al., (2008)

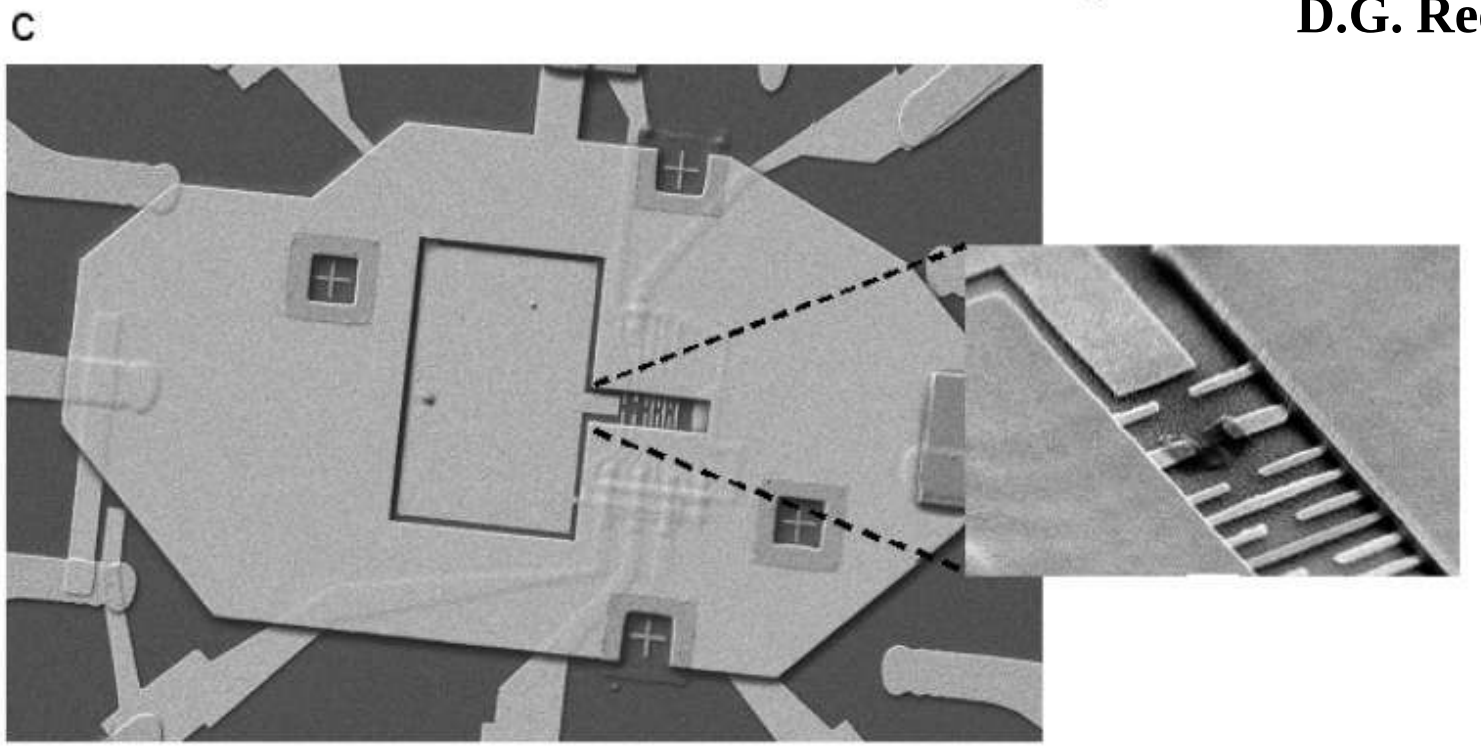

Efficient clocked electron transfer on superfluid helium

[F.R. Bradbury et al., PRL 107, 266803 (2011)]

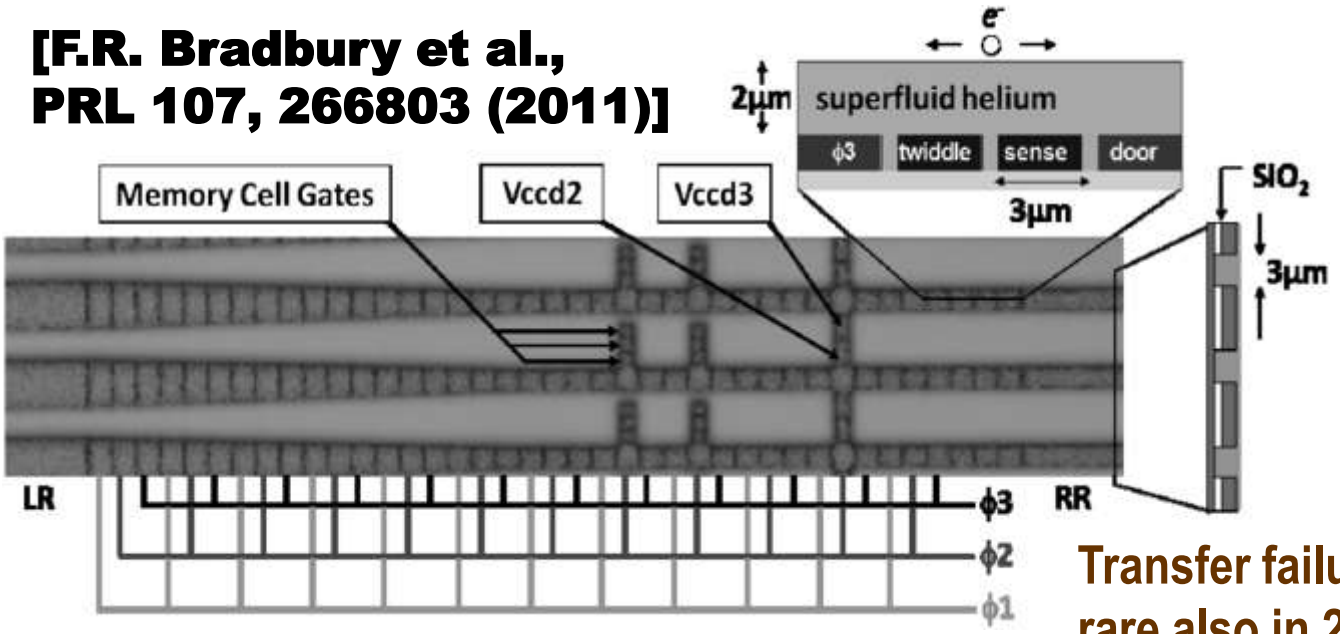

Unprecedented transport efficiency of 0.9999999999, at least by 4 orders higher than in semiconductor devices, is demonstrated for electrons on the surface of micron-scale superfluid helium-filled channels.

Transfer failures are undetectably rare also in 2D after >billion cycles

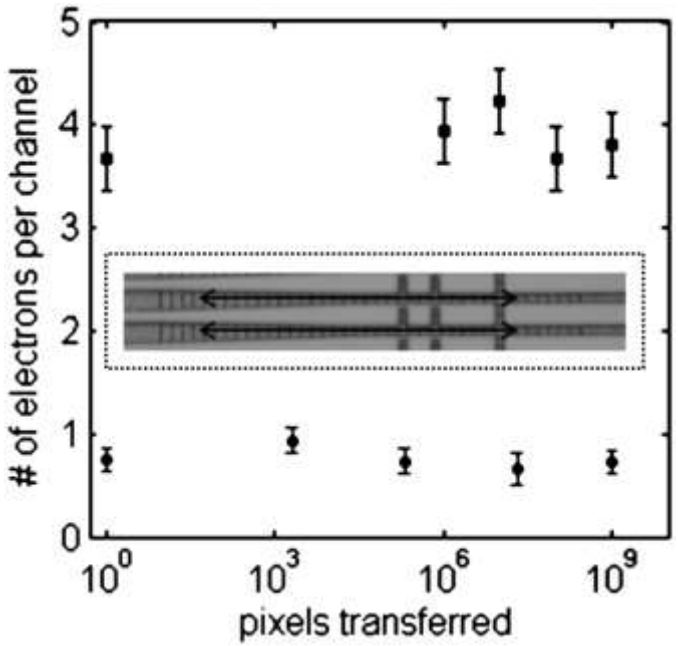

This extremely efficient transport is measured in 120 channels simultaneously with packets of up to 20 electrons, and down to singly occupied pixels. These results point the way towards the large scale transport of computational qubits, used for communications in a hybrid qubit system.

Conclusion: extremely efficient transport allows interaction between remote qubits, which increases the number of qubits in QC

Experiments with qubits in quantum dots in semiconductors

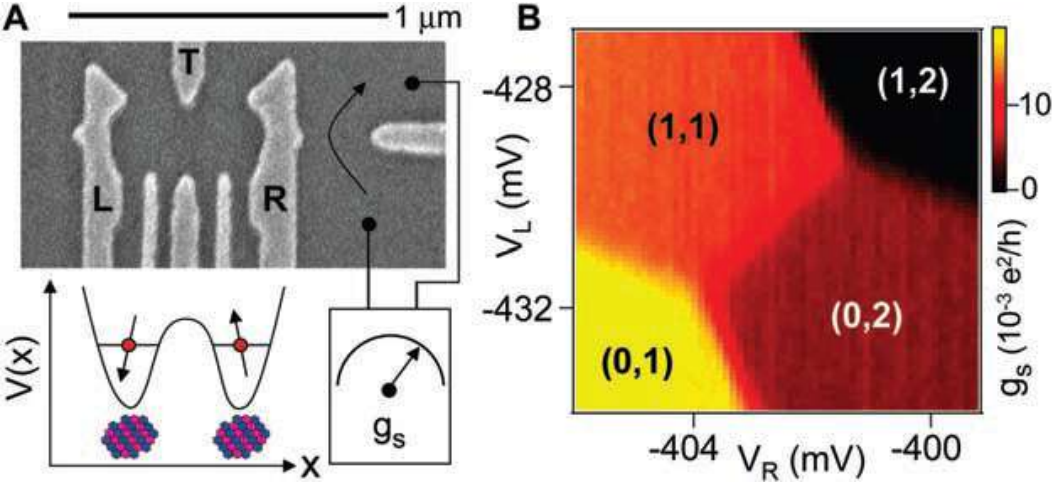

Fig. 1 (A) Scanning electron micrograph of a sample consisting of electrostatic gates on the surface of a 2D electron gas. Voltages on gates L and R control the number of electrons in the left and right dots. Gate T is used to adjust the interdot tunnel coupling. (B) conductance g_s measured as a function of V_L and V_R reflects the double-dot charge stability diagram. Charge states are labeled (m,n), where m(n) is the number of electrons in the left(right) dot.

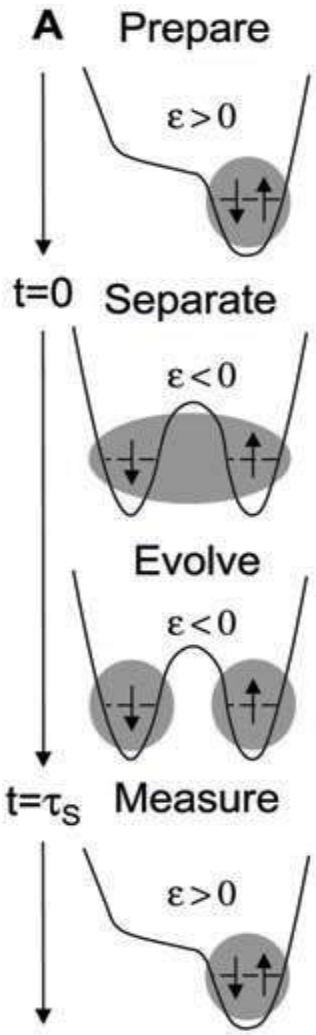

Fig.2 Control cycle for experiments consists of preparation, singlet separation, evolution of various kinds, and projection onto the (0,2) singlet state (measurement). Measurement is based on the spin-blockaded transition of T states onto (0,2)S, whereas S states proceed freely, allowing S to be distinguished from T by the charge sensor.

J. R. Petta *et al.*, Science 309, 2180 (2005);

A.C. Johnson *et al.*, Nature 435, 925 (2005); D.P. DiVincenzo, Science 309, 2173 (2005), etc

Similar spin-qubits in QD on He surface are more efficient !

Conclusions

1). Electrons on liquid helium surface are very attractive for physical realization of qubit. They have extremely long coherence time: τ >100s for spin qubits and τ >100μs for charge qubits. In addition, unprecedented transport efficiency can be achieved with electrons on He surface, which facilitates interaction between remote qubits and makes accessible many-qubit quantum computations. The read-out process is simple for charge qubits and also possible for spin-qubits.

2). The standard 2D electronic devices, such as quantum dots, filaments, charge-coupled devices, etc. can be placed on a substrate under He film and used for manipulations with electrons on liquid He surface (no need to fabricate anew). Some methods/equipment developed for measuring surface electron states in solids may also be useful for study surface electrons states above liquid helium. Qubits based on electrons (or negative ions) on He surface are much more efficient than qubits on quantum dots in semiconductors and similarly feasible.

3) The electrons on liquid He surface are very promising for physical realization of quantum computing but have received unfairly little attention so far.

Thank you for your attention!

Appendix

Atoms on the surface quantum level (surfons)

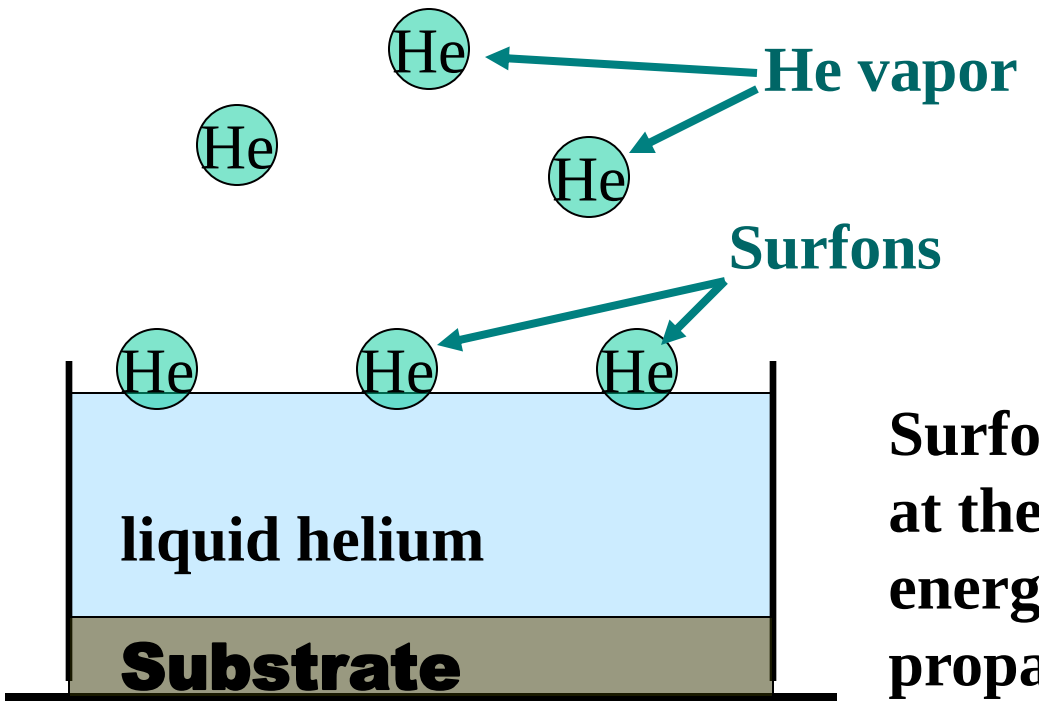

Temperature dependence of the surface tension $\Delta\sigma(T)$ of both He isotopes can be explained if we introduce a new type of excitations – surfons.

Surfon is a bound state of an atom at the surface, which has lower energy than He vapor and can propagate along the surface

Surfons interact with surface electrons. On He this interaction is weak because of small overlap of electron and surfon wave functions. However, above solid hydrogen this interaction explains the shift and width of electron transitions.

A.M. Dyugaev and P.D. Grigoriev, JETP Lett.78, 466 (2003).
A.D. Grigoriev, P.D. Grigoriev, A.M. Dyugaev, J. Low Temp. Phys. 163, 131–147 (2011)
P.D. Grigor'ev, A.M. Dyugaev, E.V. Lebedeva, JETP Lett. 87, 106 (2008); JETP 104, 1, (08)

Surface tension of liquid ^{4}He and ^{3}He, theory and experiment.

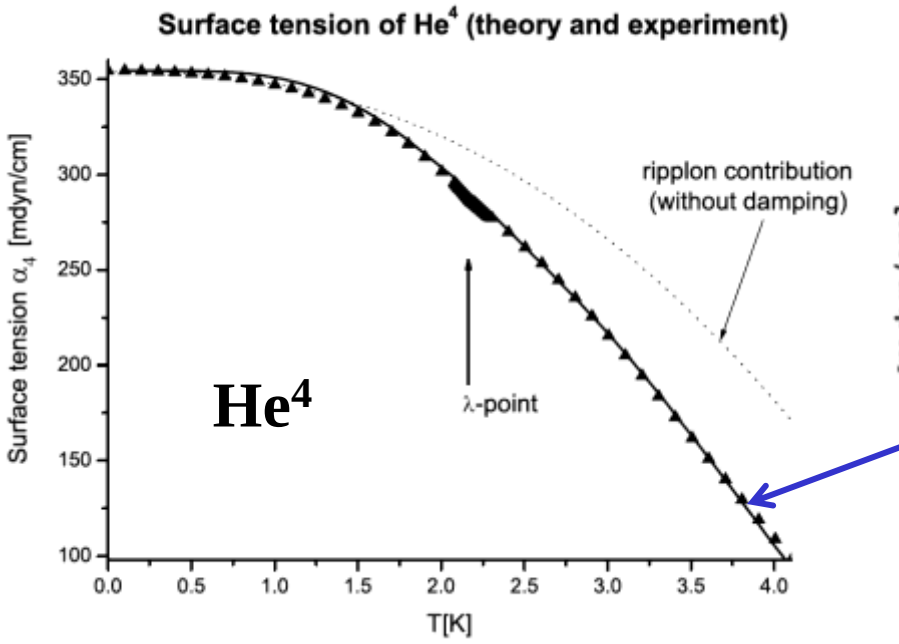

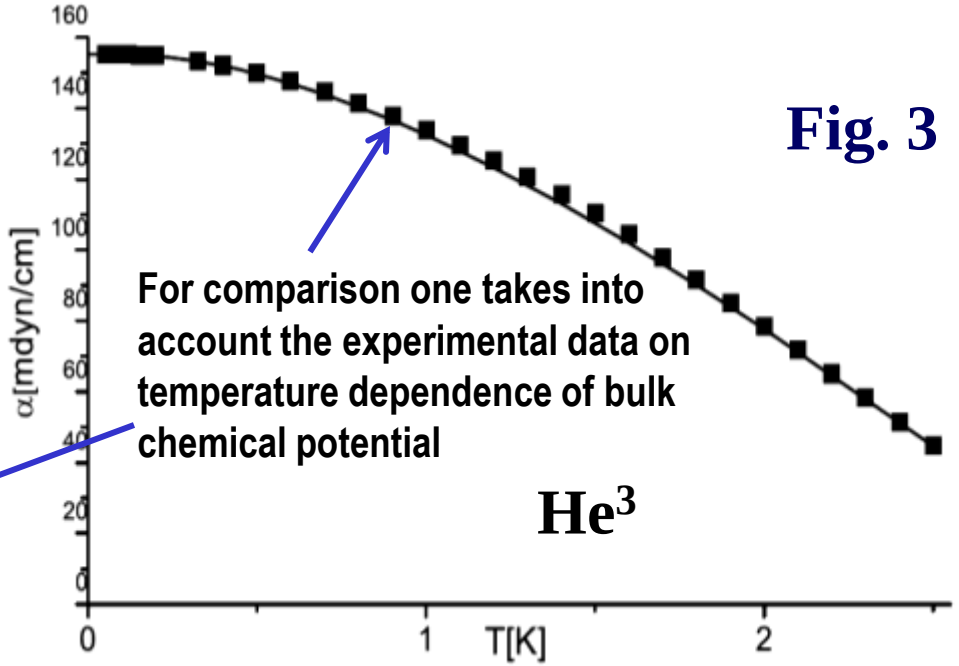

Fig. 3

For comparison one takes into account the experimental data on temperature dependence of bulk chemical potential

There is one fitting parameter – the effective mass of surfons, which determines their DOS. Another fitting parameter – activation energy □ is fixed by low-T part: $E_s^{He4} \approx -4.5$ K and $E_s^{He3} \approx -2.25$ K.

$$M_4^* \approx 2.65 M_4^0, \quad \text{and} \quad M_3^* \approx 2.25 M_3^0,$$

$$M_4^* \approx M_4^0(1 + n_{He4} V_{4d}) = 2.04 M_4^0.$$

$$M_3^* \approx M_3^0(1 + n_{He3} V_{3d}) = 2.23 M_3^0.$$

The best fit gives the effective masses
Estimated surfon effective mass is slightly less than that giving the best fit.

A.D. Grigoriev, A.M. Dyugaev, P.D. Grigoriev, J. Low Temp. Phys. 163, 131–147 (2011).

Surface tension of ^{4}He

Density of surfons increase with temperature:

$$n_4(T)=\int\frac{d^2p}{(2\pi)^2}\left[\exp\left(\frac{\varepsilon_4(p)-\mu_4}{T}\right)-1\right]^{-1},\ \varepsilon_4(p)=\Delta_4+\frac{p^2}{2m_4}$$

The surface tension $\sigma_4(T)=\sigma_4(0)+\sigma_4^R(T)+\Omega_4^S(\mu_4,T),$

where ripplon contribution $\sigma_4^R(T)=-AT^{7/3}$ **(Atkins, 1953)**

and the surface atoms contribution

$$\Omega_4(T)=-T\int\frac{d^2p}{h^2}\ln\left[1-\exp\left(\frac{\mu_4-\varepsilon_4(p)}{T}\right)\right]=-\frac{4\pi M_4T^2}{h^2}\int_0^\infty\frac{x\,dx}{\exp\left(x+\frac{\Delta_4}{T}\right)-1}.$$

A.M. Dyugaev, P.D. Grigoriev, JETP Lett.78(7), 466 (2003).

Surface tension of ^{3}He

Density of surfons increase with temperature:

$$n_3(T) = 2\int \frac{d^2p}{h^2}\left[\exp\left(\frac{\varepsilon_3(p)-\mu_3}{T}\right)+1\right]^{-1},\ \varepsilon_3(p) = \Delta_3 + \frac{p^2}{2m_3}$$

The surface tension $\sigma_3(T) = \sigma_3(0) + \Omega_3(\mu_3, T),$

where $\Omega_3(T) = -2T\int \frac{d^2p}{(2\pi)^2}\ln\left[1+\exp\left(\frac{\mu_3-\varepsilon_3(p)}{T}\right)\right].$

$$\sigma_3(T) = 155.3 - 61.2T^2\int_0^\infty \frac{xdx}{\exp\left(x+\frac{\Delta_3}{T}\right)+1}$$

A.M. Dyugaev, P.D. Grigoriev, JETP Lett.78(7), 466 (2003).

Fig. 3

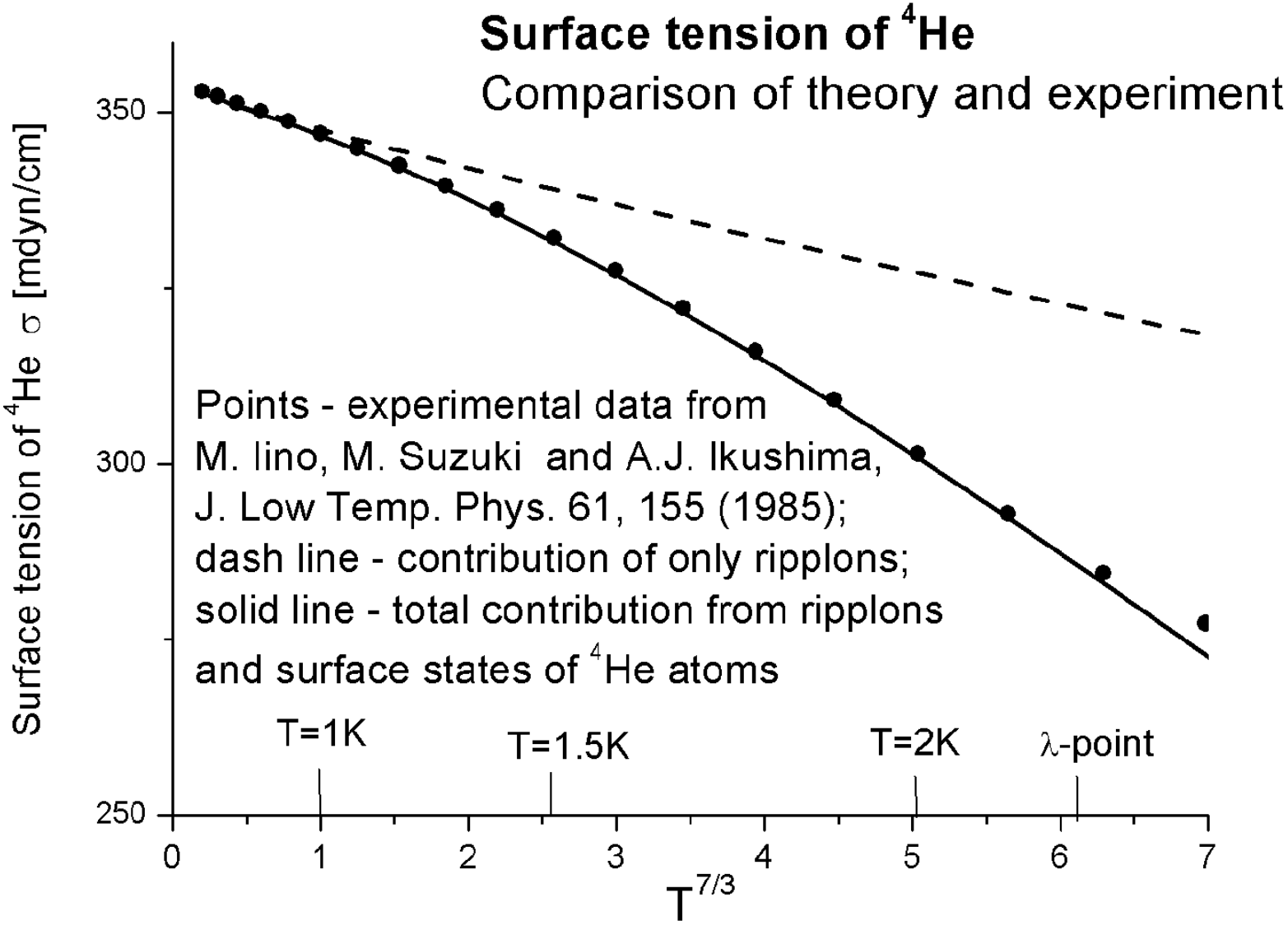
Surface tension of ^{4}He
Comparison of theory and experiment
Surface tension of ^{4}He σ [mdyn/cm]
350
300
250
Points - experimental data from
M. Iino, M. Suzuki and A.J. Ikushima,
J. Low Temp. Phys. 61, 155 (1985);
dash line - contribution of only ripplons;
solid line - total contribution from ripplons
and surface states of ^{4}He atoms
T=1K
T=1.5K
T=2K
λ-point
0
1
2
3
4
5
6
7
$T^{7/3}$

Fig. 1

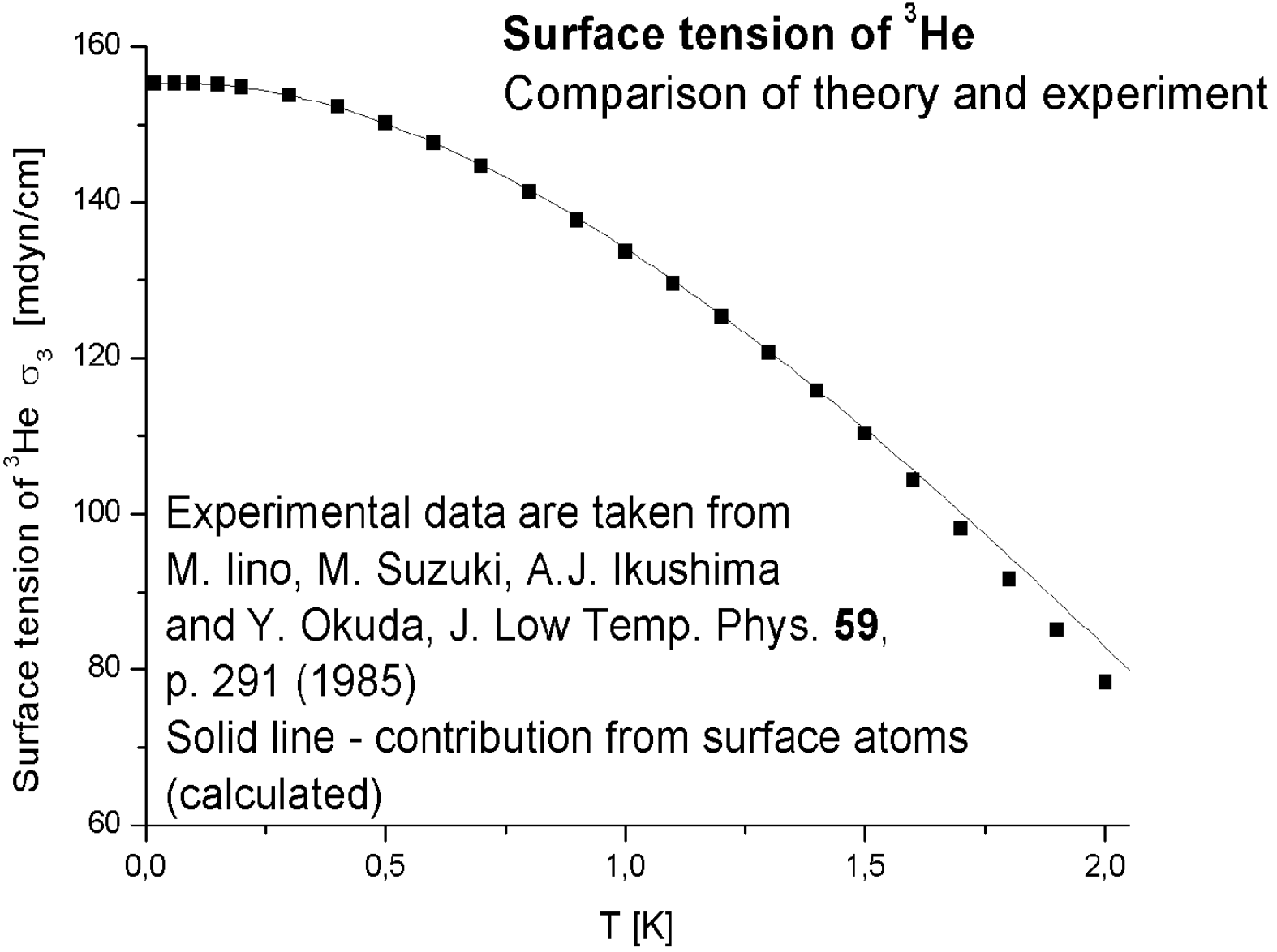
Surface tension of ^{3}He
Comparison of theory and experiment
Surface tension of ^{3}He σ_3 [mdyn/cm]
160
140
120
100
80
60
0,0
0,5
1,0
1,5
2,0
T [K]
Experimental data are taken from
M. Iino, M. Suzuki, A.J. Ikushima
and Y. Okuda, J. Low Temp. Phys. **59**,
p. 291 (1985)
Solid line - contribution from surface atoms
(calculated)

Fig. 2

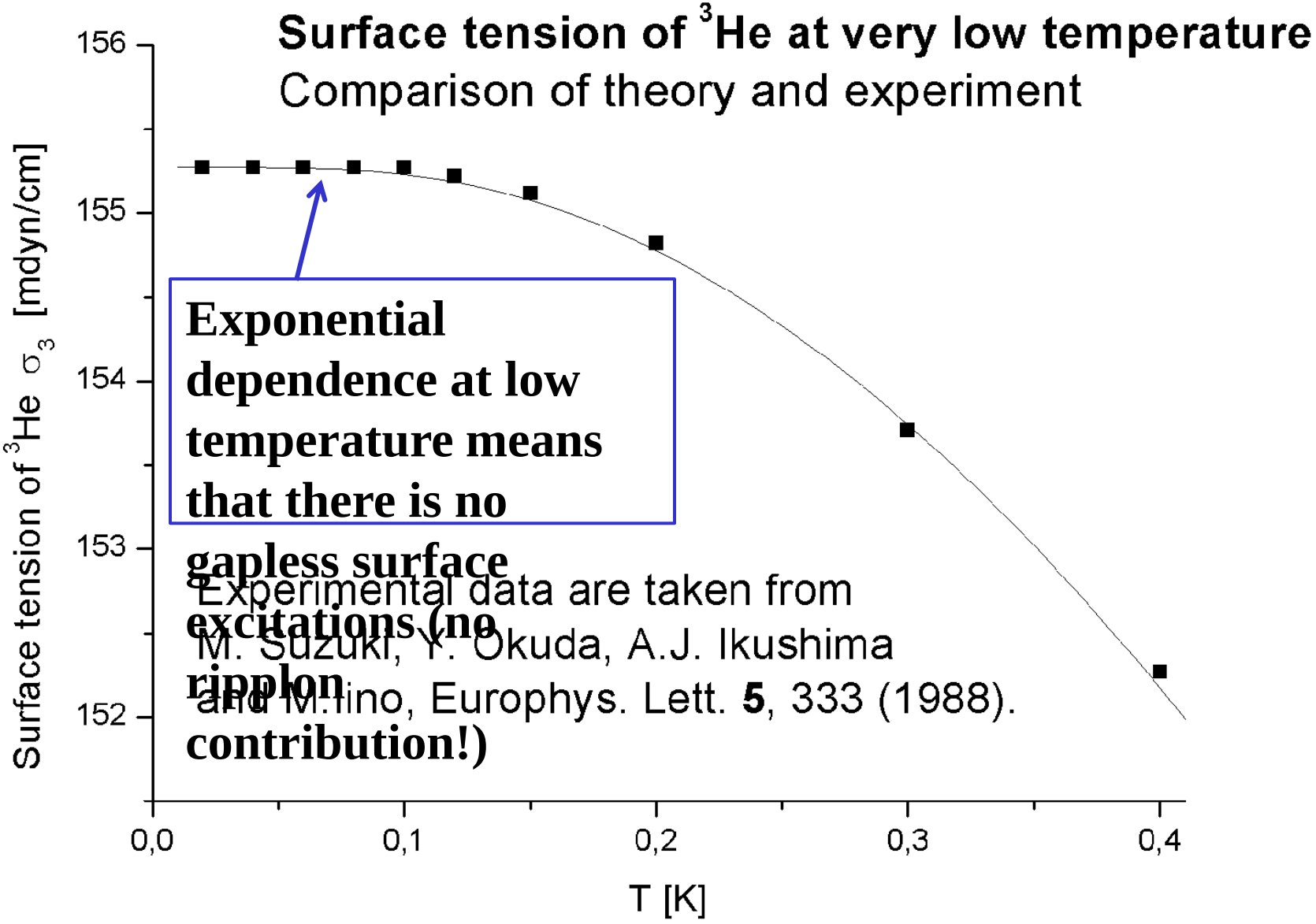
Surface tension of ^{3}He at very low temperature
Comparison of theory and experiment
Surface tension of ^{3}He σ_3 [mdyn/cm]
156
155
154
153
152
0,0
0,1
0,2
0,3
0,4
T [K]
Exponential dependence at low temperature means that there is no gapless surface excitations (no ripplon contribution!)
Experimental data are taken from
M. Suzuki, Y. Okuda, A.J. Ikushima
and M.Iino, Europhys. Lett. 5, 333 (1988).

Various energy levels of surface electrons

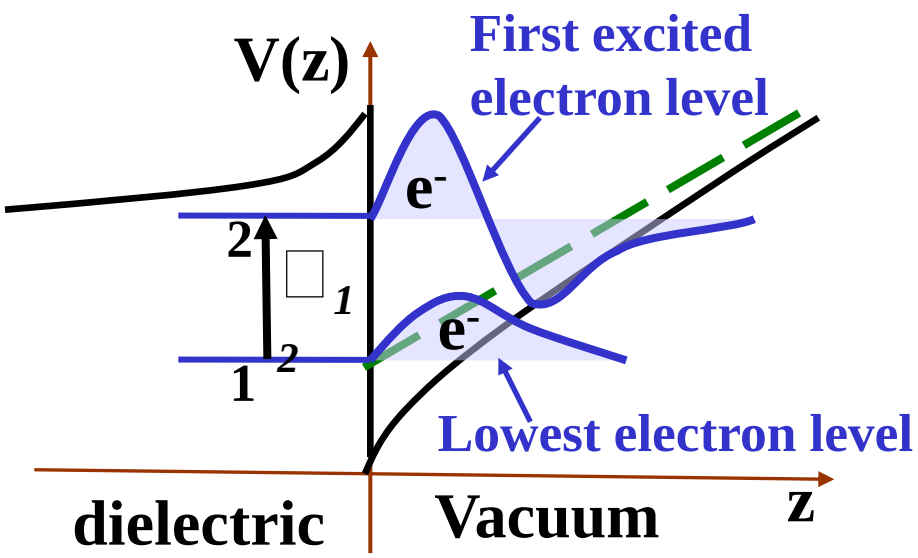

Electron transitions between different energy levels above the surface can be measured.

The position and width of the transition line depends on T!

[V.V. Zav'yalov, I.I. Smol'yaninov, JETP Lett. 44, 182 (1986)]

Quantum transitions of electrons on the surface

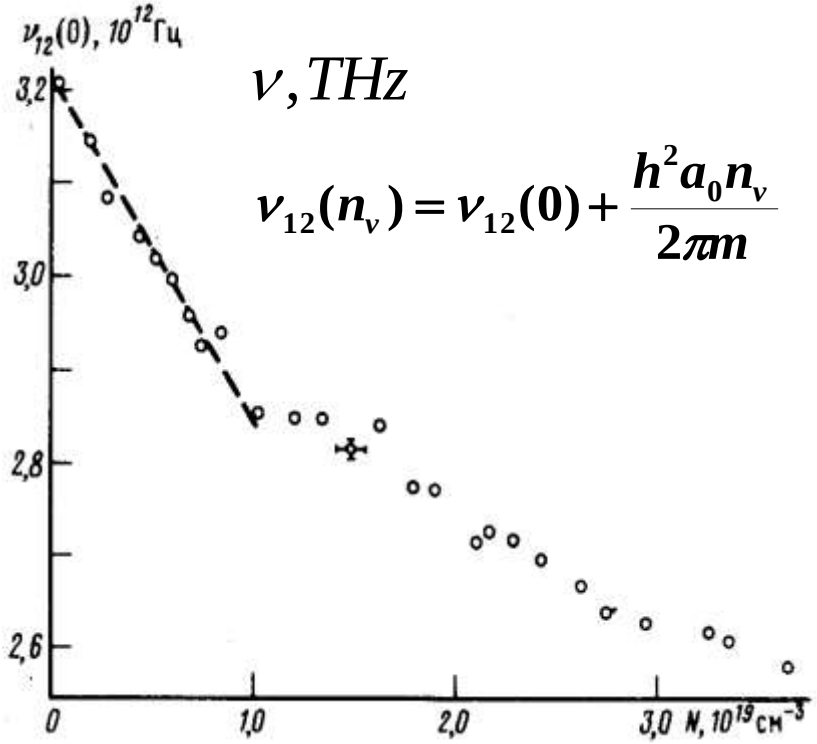

$$\nu, THz$$

$$\nu_{12}(n_\nu) = \nu_{12}(0) + \frac{h^2 a_0 n_\nu}{2\pi m}$$

Experimental data from : V.V. Zav'yalov, I.I. Smol'yaninov, JETP Lett. 44, 182 (1986); Sov. Phys. JETP 65, 194 (1987); ibid 67, 171 (1988).

The temperature dependence of the shift of the frequency of electron transition 1->2 plotted as function of the vapor density N_V

$$N(T) \propto \exp(-|\mu|/k_B T),\ |\mu| \approx 92K$$

does not fit the line $\Delta E_n = \frac{2\pi\hbar^2}{m} a_0 n_\nu$, **theoretical prediction**

If one applies the linear fit of $\nu_{12}(n_V)$ the obtained value

$$a_0 = -1.4\,A$$

The accepted value, obtained from atomic scattering experiments, has different sign:

$$a_0 = 0.67\,A$$

This disagreement suggests that the hydrogen vapor only does not explain of the temperature shift of transition frequency

Quantum transitions of electrons on the surface shifted due to the interaction with surfons. The shift depends on T

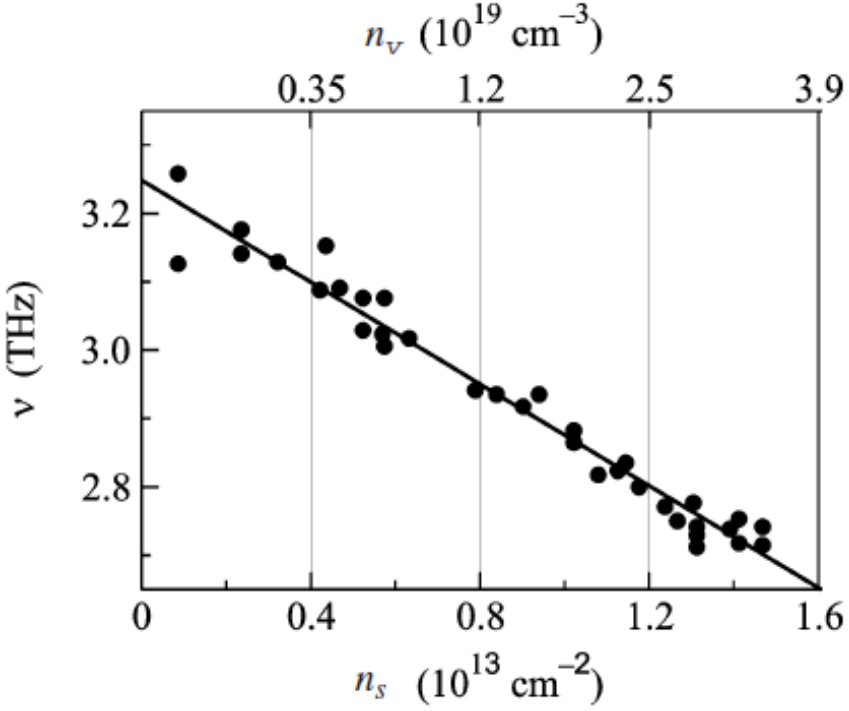

Experimental data from : V.V. Zav'yalov, I.I. Smol'yaninov, JETP Lett. 44, 182 (1986); Sov. Phys. JETP 65, 194 (1987); ibid 67, 171 (1988).

The shift of electron transition line is linear as function of surfon density n_S

P. D. Grigor'ev, A. M. Dyugaev and E. V. Lebedeva, JETP Lett. 87, 106 (2008).

This shift gives a strong proof of the existence of surfons !

The surfons exist not only on helium or hydrogen surfaces, but in all cryogenic liquids.

Calculation of the shift of electron energy levels due to electron interaction with surfons

The shift of the n-th electron energy level is given by

$$E_n = E_{n0} + \Delta E_n, \quad \Delta E_n = \frac{h^2 a_0}{2\pi m}\int_0^\infty \varphi_{n0}^2(z) n_v(z) dz, \quad \int_0^\infty \varphi_{n0}^2 dz = 1$$

where a_0 is the scattering amplitude of electron by vapor atom.

The uniform distribution of vapor along z-axis produces the same shift of different electron energy levels

! The temperature-dependent shift of interlevel electron transition line may only come from non-uniform vapor

$$E_n - E_1 = E_{n0} - E_{10} - \frac{h^2 a_0}{2\pi m}\int_0^\infty (\varphi_{10}^2 - \varphi_{n0}^2)(n_v(z) - n_{v\infty}) dz$$

Calculation of the shift of electron energy levels due to electron interaction with surfons

The z-dependent vapor density leads to the shift of electron transition line:

$$E_n - E_1 = E_{n0} - E_{10} - \delta n_s$$

$$\delta = \frac{h^2 a_0}{2\pi m}\left[\varphi_{10}^2(z_0) - \varphi_{n0}^2(z_0)\right]$$

$$\varphi_{10}^2 = \frac{4z^2}{r_e^3}\exp(-2z/r_e)$$

$$\varphi_{20}^2 = \frac{z^2}{2r_e^3}\exp(-z/r_e)\left(1 - \frac{z}{2r_e}\right)$$

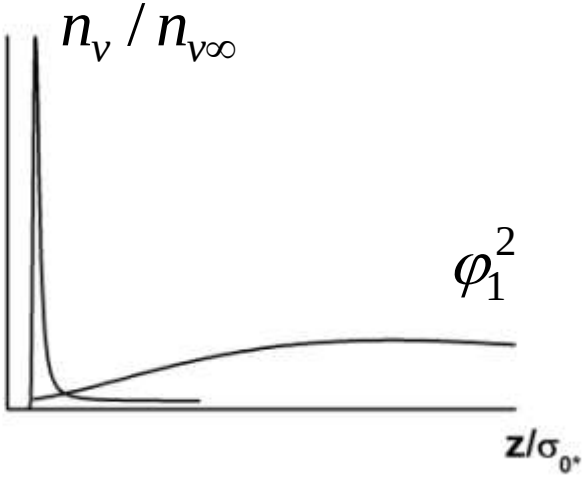

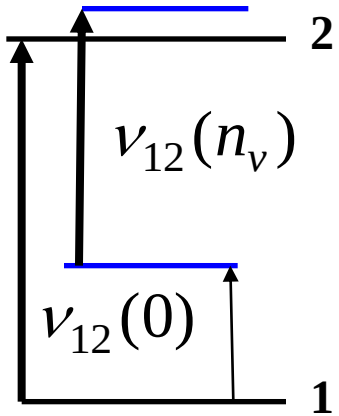

Now the ground state is shifted stronger ⇨ **scattering length has positive sign** $a_0 > 0$

Contribution of surface level atoms to the electron scattering

Inverse scattering time is related to the He atom density *n(z)* above the surface

$$\frac{1}{\tau} = \int dz\, \Psi_e^4(z) n_{He}(z) \frac{Ah}{\pi m}.$$

where A is the scattering amplitude.

This He atom density *n(z)* contains vapor atoms and surfons.

Electron mobility $\eta = \tau / m.$

One can expect to answer another long-standing question: why the electron mobility on liquid helium surface is ~2 times smaller than the theoretical prediction.

Other experiments, indicating the existence of surfons

Mobility of surface electrons above liquid helium.

The scattering rate of surface electrons on He vapor is not enough (~2 times) to explain the low electron mobility. The scattering by surfons considerably improves the agreement (by a factor of ~1.5) but still not enoug

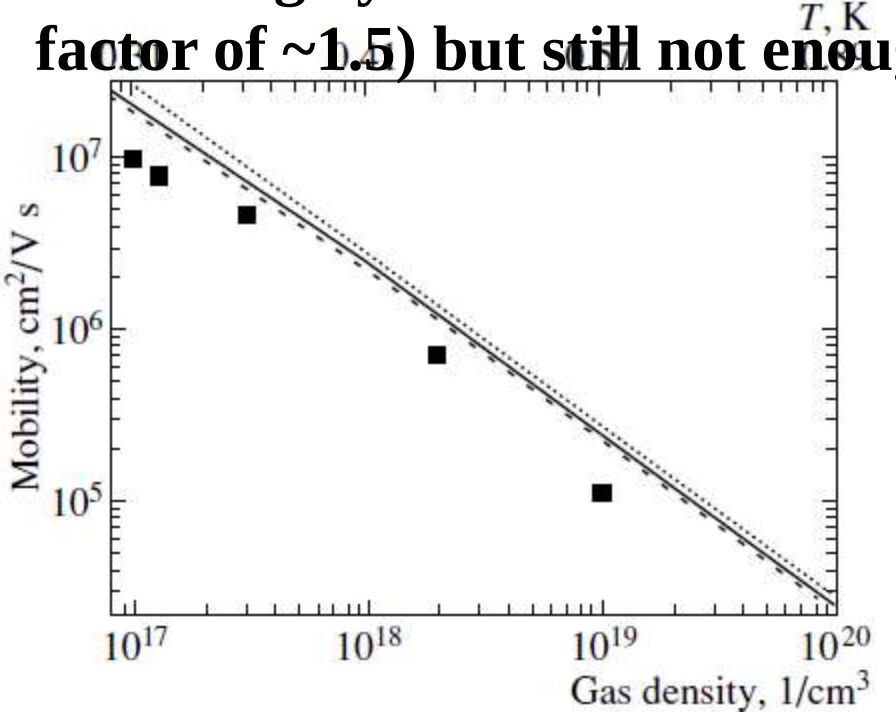

The electron-surfon interaction above liquid helium is weak because of small overlap of electron and surfon wave functions. The result is very sensitive to the exact shape of surfon Ψ(z).

[P.D. Grigoriev, A.M. Dyugaev, E.V. Lebedeva, "Electron mobility on a surface of dielectric media: influence of surface level atoms", JETP 104 (1), p. 1-

First difficulty: decoherence

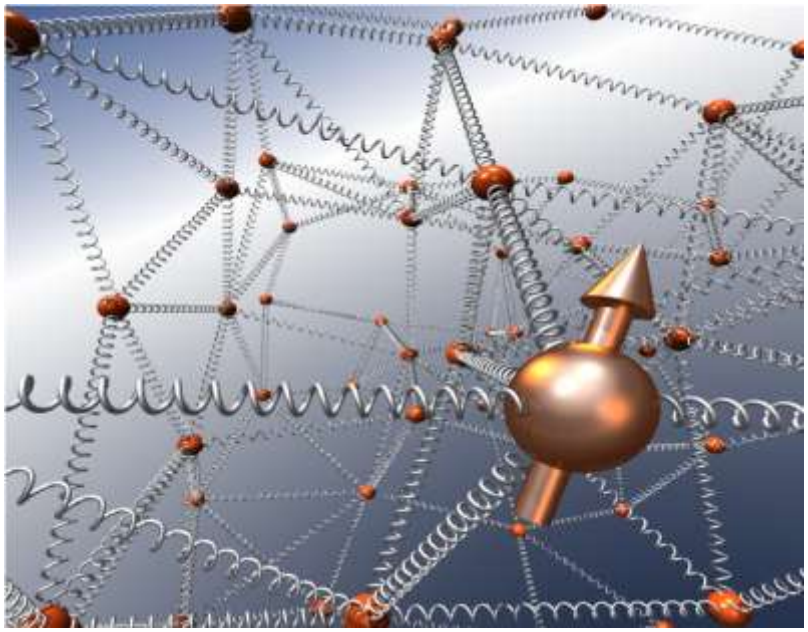

Decoherence (the qubit lifetime" is limited) => inevitable errors.

The Shor factorization algorithm of L-digit number needs ~L^3 operations + ~L qubits, => needs $\tau_{dc}/\tau_{op} > L^4$.

Error-correction is useful if at least 10^4 coherent operations are possible.

This means that at least 10^4 Rabi oscillations in a qubit must be possible before decoherence !

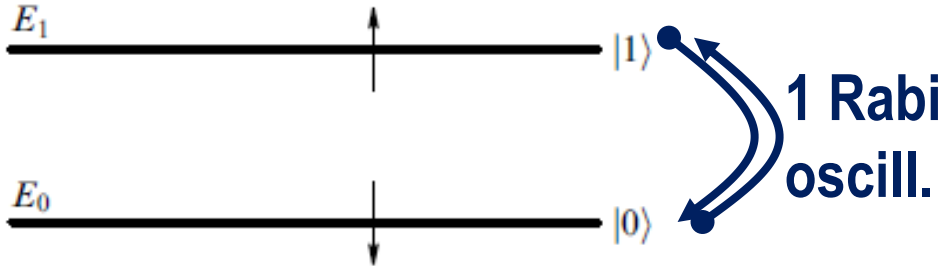

<u>Other difficulties</u>: read-off and controllable interaction between qubits.